Article

Cell Reports

Nucleosome Assembly Dynamics Involve Spontaneous Fluctuations in the Handedness of Tetrasomes

Graphical Abstract

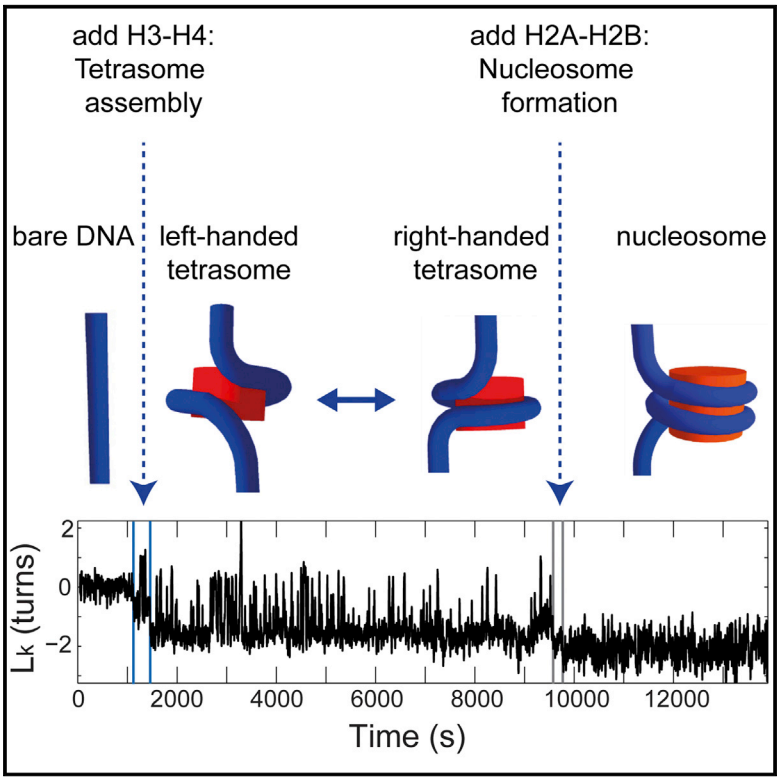

Authors

Rifka Vlijm, Mina Lee, ..., Cees Dekker, Nynke H. Dekker

Correspondence

c.dekker@tudelft.nl (C.D.),
n.h.dekker@tudelft.nl (N.H.D.)

In Brief

In eukaryotes, DNA is wrapped in a left-handed fashion around histone protein cores, forming nucleosomes. Vlijm et al. now use real-time monitoring of DNA length and linking number to show that tetrasomes, biologically relevant subnucleosomal structures, exhibit spontaneous flipping between a preferentially occupied left-handed and a right-handed state.

Highlights

- We monitor assembly of nucleosomes and tetrasomes by NAP1 on DNA in real time
- Tetrasomes spontaneously flip between a left- and right-handed conformation
- Addition of H2A/H2B to flipping tetrasomes generates stable left-handed nucleosomes
- Small positive torques drive tetrasomes from a left-handed into a right-handed state

Vlijm et al., 2015, Cell Reports *10*, 1–10
January 13, 2015
http://dx.doi.org/10.1016/j.celrep.2014.12.022

CellPress

Please cite this article in press as: Vlijm et al., Nucleosome Assembly Dynamics Involve Spontaneous Fluctuations in the Handedness of Tetrasomes, Cell Reports (2015), http://dx.doi.org/10.1016/j.celrep.2014.12.022

Cell Reports
Article

Nucleosome Assembly Dynamics Involve Spontaneous Fluctuations in the Handedness of Tetrasomes

Rifka Vlijm,[1,3] Mina Lee,[1,3] Jan Lipfert,[1,4] Alexandra Lusser,[2] Cees Dekker,[1,*] and Nynke H. Dekker[1,*]
[1]Department of Bionanoscience, Kavli Institute of Nanoscience, Delft University of Technology, Lorentzweg 1, 2628 CJ Delft, the Netherlands
[2]Division of Molecular Biology, Biocenter, Innsbruck Medical University, Innrain 80-82, 6020 Innsbruck, Austria
[3]Co-first author
[4]Present address: Department of Physics and Center for Nanoscience (CeNS), Ludwig-Maximilian-University, Amalienstrasse 54, 80799 Munich, Germany
*Correspondence: c.dekker@tudelft.nl (C.D.), n.h.dekker@tudelft.nl (N.H.D.)
http://dx.doi.org/10.1016/j.celrep.2014.12.022

SUMMARY

DNA wrapping around histone octamers generates nucleosomes, the basic compaction unit of eukaryotic chromatin. Nucleosome stability is carefully tuned to maintain DNA accessibility in transcription, replication, and repair. Using freely orbiting magnetic tweezers, which measure the twist and length of single DNA molecules, we monitor the real-time loading of tetramers or complete histone octamers onto DNA by Nucleosome Assembly Protein-1 (NAP1). Remarkably, we find that tetrasomes exhibit spontaneous flipping between a preferentially occupied left-handed state ($\Delta Lk = -0.73$) and a right-handed state ($\Delta Lk = +1.0$), separated by a free energy difference of 2.3 k_BT (1.5 kcal/mol). This flipping occurs without concomitant changes in DNA end-to-end length. The application of weak positive torque converts left-handed tetrasomes into right-handed tetrasomes, whereas nucleosomes display more gradual conformational changes. Our findings reveal unexpected dynamical rearrangements of the nucleosomal structure, suggesting that chromatin can serve as a "twist reservoir," offering a mechanistic explanation for the regulation of DNA supercoiling in chromatin.

INTRODUCTION

Nucleosomes, the basic compaction unit of eukaryotic DNA (Kornberg, 1977; Olins and Olins, 1974), consist of 147 bp of DNA wrapped 1.7 times around a protein core called the histone octamer (Luger et al., 1997). Their assembly requires a precisely defined pathway: first two copies of the H3-H4 histones bind to the DNA, forming a tetrasome, followed by the two H2A-H2B dimers (Jorcano and Ruiz-Carrillo, 1979). In vivo, nucleosome assembly is facilitated by chaperones, such as NAP1 (Andrews et al., 2010; Ito et al., 1996; Zlatanova et al., 2007) and ATP-dependent chromatin-assembly factors (Lusser et al., 2005). In vitro, nucleosome assembly onto DNA fragments is often carried out using salt dialysis (Peterson, 2008). It has been established that nucleosome positioning is sensitive to the DNA sequence, with the binding affinity for a given 147 bp sequence varying over more than three orders of magnitude (Thåström et al., 1999). High-affinity binding to DNA sequences that contain 10 bp repeats of bendable AT/TA dinucleotides (Jiang and Pugh, 2009; Kaplan et al., 2009; Struhl and Segal, 2013; Zhang et al., 2009) has facilitated both high-throughput visualization of nucleosomes (Lee and Greene, 2011; Visnapuu and Greene, 2009) and the mapping out of the energy landscape for single nucleosomes or nucleosome arrays through mechanical disruption (Brower-Toland et al., 2002; Hall et al., 2009; Bancaud et al., 2007; Kruithof et al., 2009), providing quantitative insight into the underlying histone-DNA interactions.

It is becoming increasingly clear that nucleosomes exhibit structural dynamics that are key to understanding the mechanisms regulating genome accessibility in transcription, replication, and repair (Bell et al., 2011; Choy and Lee, 2012; Gansen et al., 2009; Simon et al., 2011; Zentner and Henikoff, 2013). For example, nucleosomes display dynamical "breathing" (Li et al., 2005), in which short stretches of DNA transiently unwrap from the octamer. In addition, active remodeling of nucleosomes alters their stability and positioning (Blosser et al., 2009; Clapier and Cairns, 2009). Several studies suggest that altered conformations of nucleosomes and tetrasomes may be associated with changes in the topology of the wrapped DNA (Bancaud et al., 2007; Hamiche et al., 1996; Peterson et al., 2007), which could have profound implications for cellular processes like transcription and replication (Liu and Wang, 1987). To date, however, no studies have addressed the dynamics of (sub)nucleosome chirality, which requires the ability to detect transient states in nucleosomal linking number.

Here, we directly monitor, in real time, the NAP1-mediated assembly of (sub-)nucleosomes onto bare DNA and its subsequent dynamics. In vivo, NAP1 has been found to predominantly interact with H2A/H2B and is considered responsible for the loading of H2A/H2B onto chromatin (Zlatanova et al., 2007). In vitro, NAP1 prevents histone aggregation and acts as a chaperone for both H2A/H2B and H3/H4, facilitating their stepwise loading onto DNA that is free of any strong positioning sequences that could impact subsequent dynamics (Andrews

Please cite this article in press as: Vlijm et al., Nucleosome Assembly Dynamics Involve Spontaneous Fluctuations in the Handedness of Tetrasomes, Cell Reports (2015), http://dx.doi.org/10.1016/j.celrep.2014.12.022

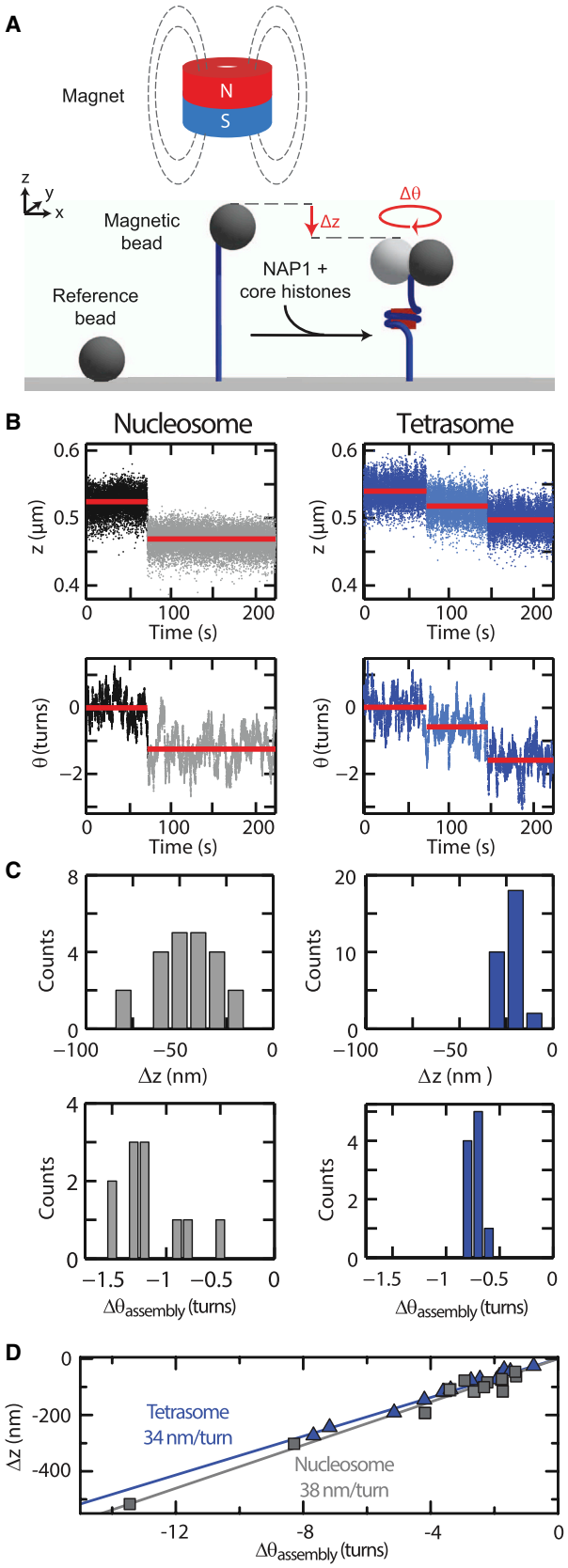

Figure 1. NAP1-Assisted Nucleosome and Tetrasome Assembly

(A) Schematic of the in vitro single-molecule assay showing a DNA molecule (blue) tethered between a glass surface and a paramagnetic bead in the FOMT. The circular magnet above the bead applies a stretching force on the DNA. In contrast to conventional magnetic tweezers (Strick et al., 1996), no rotational clamp is imposed, and the bead is free to rotate about the DNA-tether axis. A nonmagnetic reference bead is fixed to the surface to allow for drift correction. After flushing in NAP1 and appropriate core histones (main text), either nucleosomes or tetrasomes can be loaded onto the DNA. We maintained all histone concentrations at low levels to ensure the assembly of only one or a few nucleosomes (Experimental Procedures).

(B) Time dependence of the end-to-end length z (μm) (top) and bead rotations θ (turns) (bottom) of a single DNA tether during the assembly of a single nucleosome (left, black/ gray data) or two tetrasomes (right, blue data). Compaction of the DNA (decrease in z) occurs concurrently with a change in linking number (changes in θ). Data were acquired at 100 Hz, and red lines indicate the mean values of each assembly step.

(C) Histograms of the step sizes in extension, Δz, and in linking number, $\Delta\theta_{assembly}$, during nucleosome (gray, left) and tetrasome (blue, right) assembly. On average, the assembly of a single nucleosome (tetrasome) results in a compaction of the DNA length by 46 ± 16 nm (24 ± 3 nm) and a simultaneous change in the linking number by −1.2 ± 0.3 (−0.73 ± 0.05). The histograms contain fewer steps in θ compared to steps in z, because not all assembly events were sufficiently temporally separated (with respect to the temporal resolution of the angular coordinate) to properly determine $\Delta\theta$. Although typically nucleosomes assembled in a single correlated step in z and θ, occasionally two smaller correlated steps were required (Vlijm et al., 2012), as reflected by the spread in the histograms of both step sizes (left panels).

(D) Plot of the total amount of compaction (Δz) versus the total change in linking number ($\Delta\theta_{assembly}$) on DNA molecules following the assembly of either nucleosomes (gray squares) or tetrasomes (blue triangles). Fits to a linear relationship yield $\Delta z/\Delta\theta_{assembly}$ = 38 ± 1 nm/turn (solid gray line) for nucleosomes and $\Delta z/\Delta\theta_{assembly}$ = 34 ± 1 nm/turn (solid blue line) for tetrasomes.

et al., 2010; Asahara et al., 2002; Mazurkiewicz et al., 2006; Nakagawa et al., 2001; Peterson et al., 2007; Vlijm et al., 2012). Our real-time monitoring of the dynamics of single (sub)nucleosomal structures was achieved using Freely Orbiting Magnetic Tweezers (FOMT) (Figure 1A; Lipfert et al., 2011), a technique that allows to simultaneously measure dynamical changes in the end-to-end length and linking number of single DNA molecules tethered between a flow cell surface and magnetic beads during the assembly of nucleosomes or tetrasomes onto the DNA. In this approach, a vertically oriented magnetic field is used to apply a stretching force (which we limit to 0.7 pN, well below the 3 pN above which DNA begins to peel off from the nucleosome) (Chien and van Noort, 2009), without constraining the free rotation of the DNA molecule.

Our results show that, unexpectedly, H3/H4 tetrasomes are very dynamic: they exhibit spontaneous flipping between a preferentially occupied left-handed state with ΔLk = −0.73, and right-handed state with ΔLk = +1.0, without concomitant changes in DNA end-to-end length. We demonstrate that such dynamically flipping tetrasomes can, through the subsequent addition of H2A/H2B dimers, continue to form proper nucleosomes with the DNA wound in a left-handed path, and we propose a molecular model for the sequence of protein conformational changes that contribute to the overall change in tetrasome handedness. Last, we show how the application of only very weak positive torques can fully drive tetrasomes from left- into right-handed states, thereby suggesting how the conformational changes undergone by tetrasomes can be

used to prevent local buildup of torsional stress in cellular processes.

RESULTS

NAP1-Assisted Assembly of Nucleosomes and Tetrasomes

To study the formation of nucleosomes in real time, 1.9 or 3.4 kilo-base-pair (kbp) DNA molecules that did not contain specific nucleosome-positioning sequences were individually tethered in a flow cell. Using FOMT, we directly monitored nucleosome formation upon flushing core histones that had been preincubated with the histone chaperone NAP1 into the flow cell. In our single-molecule FOMT setup, we observed a distinct decrease in the end-to-end length z of the DNA upon flushing in of NAP1/histone complexes, indicating compaction, accompanied by a clockwise rotation θ of the bead, reflecting a decrease in the linking number of the DNA tether (Figure 1B, left). We obtained an average extension change $< \Delta z > = -46 \pm 16$ nm and linking number change $< \Delta\theta_{assembly} > = -1.2 \pm 0.3$ turns (Figure 1C, left; n = 8). These numbers are in good agreement with those obtained when nucleosome assembly proceeds via salt dialysis (Brower-Toland et al., 2002; Claudet et al., 2005) and indicate that NAP1 is capable of assembling complete nucleosomes without the addition of further ATP-dependent factors. We note that earlier findings that reported on incomplete nucleosome assembly by NAP1 (Torigoe et al., 2011) may have been influenced by NAP1's ability to disassemble nucleosomes when present at high concentrations (Okuwaki et al., 2010; Park et al., 2004).

Our experiments with NAP1 preincubated with only histones H3 and H4 revealed similar, correlated steps in z and θ, however, with lower amplitudes (Figure 1B, right). We measured $< \Delta z > = -24 \pm 3$ nm, and $< \Delta\theta_{assembly} > = -0.73 \pm 0.05$ turns (Figure 1C, right; n = 10), in agreement with previous measurements of the compaction (Mihardja et al., 2006; Sivolob et al., 2000) and change in linking number associated with the loading of left-handed tetrasomes (Mihardja et al., 2006; Sivolob et al., 2000). Because only histones H3 and H4 were present, these results indicate the assembly of tetrasomes by NAP1. Control experiments showed that the presence of NAP1 alone, or NAP1 preincubated with only histones H2A/H2B did not affect either the length or the linking number of bare DNA (Figure 2A).

By changing the histone concentration, we assembled varying numbers of nucleosomes or tetrasomes. The total degree of compaction Δz and the overall change in linking number $\Delta\theta_{assembly}$ following assembly were linearly correlated with similar slopes $\Delta z/\Delta\theta_{assembly}$ for nucleosomes (38 ± 1 nm/turn) and tetrasomes (34 ± 1 nm/turn) (Figure 1D), which indicates that the conformations of the nucleosomes or tetrasomes on the DNA are independent of the number of protein complexes assembled.

Tetrasomes Exhibit Spontaneous Dynamic Changes in Linking Number

Upon monitoring the molecules after assembly, we found, strikingly, that DNA loaded with tetrasomes showed spontaneous fluctuations in the linking number (Figure 2B, right, blue). This is in stark contrast to DNA loaded with nucleosomes, where the linking number remained fixed (Figure 2B, right, gray), as it did for bare DNA (Figure 2A, top right, black). For all three cases, the respective mean extensions in z remained unaltered (Figure 2A, top left, and Figure 2B, left). We observed such flipping signatures in the linking number for every DNA molecule that was loaded with tetrasomes. When only a single tetrasome was loaded, the linking number fluctuated between only two values (Figure 3A). When DNA was loaded with multiple tetrasomes, the linking number fluctuated between multiple discrete levels (Figure 3B). Overall, we determined the linking number between any two discrete levels to be $< \Delta\theta_{flipping} > = 1.7 \pm 0.1$ turns (Figure 3C, n = 10). Individual tetrasomes are thus capable of switching between a left-handed state with a mean linking number of -0.73 ($\Delta\theta_{assembly}$) and a right-handed state with a mean linking number of +1.0. This switching behavior is intrinsic to tetrasomes and not induced by free NAP1, as indicated by the continued observation of flipping signatures in experiments in which free proteins are removed from the flow cell (Figures S1A–S1C). The absence of NAP1 interference was confirmed by additional experiments in which samples were prepared by bulk reconstitution of tetrasomes onto DNA via salt dialysis (Supplemental Experimental Procedures, following protocols similar to Luger et al., 1999). Such tetrasomes displayed quantitatively identical flipping signatures as the NAP1-assembled tetrasomes in the single-molecule setup (Figures S1D and S1E).

We analyzed the flipping of tetrasomes loaded onto DNA by NAP1 in the framework of a binomial model in which a single tetrasome occupies either the left- or right-handed states, with probabilities p and (1-p) respectively (cartoons in Figures 3A and 3B). For each experiment, we determined the relative occupancies of each state from the ratios of the respective peaks' areas in the linking number histograms (Figures 3A and 3B). The experimentally determined occupancies were fit to a binomial distribution with parameters n, the number of assembled tetrasomes, determined from the size and number of steps in z during assembly, and p, which was treated as a fitting parameter (Figure 3D, top). Fitting of p for distinct DNA molecules loaded with different numbers of tetrasomes yielded an average value of $< p > = 0.90 \pm 0.08$ (Figure 3D, bottom, blue). The value of p close to 1 indicates that tetrasomes are much more likely to occupy the left-handed state over the right-handed state; the fact that p is independent of the number of assembled tetrasomes indicates that under our experimental conditions of sparse loading the tetrasomes are independent and do not interact. The fitted values of p yield a free energy difference between the left- and right-handed states according to $\Delta G = -k_B T \ln((1/p) - 1)$ (Figure 3D, bottom, red), for which we thus find a value of 2.3 ± 0.8 k_BT. This number is in excellent agreement with the value of 2.5 $k_B T$ determined via electrophoretic mobility analysis of nucleosome populations (Hamiche et al., 1996). Quantitative analysis of the lifetimes of a tetrasome in its left- and right-handed states indicates that a tetrasome in our experimental configuration has a lifetime of $\tau_{left\text{-}handed} \sim 134$ s in the left-handed state, and $\tau_{right\text{-}handed} \sim 9.5$ s in the right-handed state (Figure S2). The ratio of these lifetimes yields a similar estimate for ΔG of 2.6 ± 0.8 $k_B T$. Additionally, through the use of an Arrhenius relationship, the values

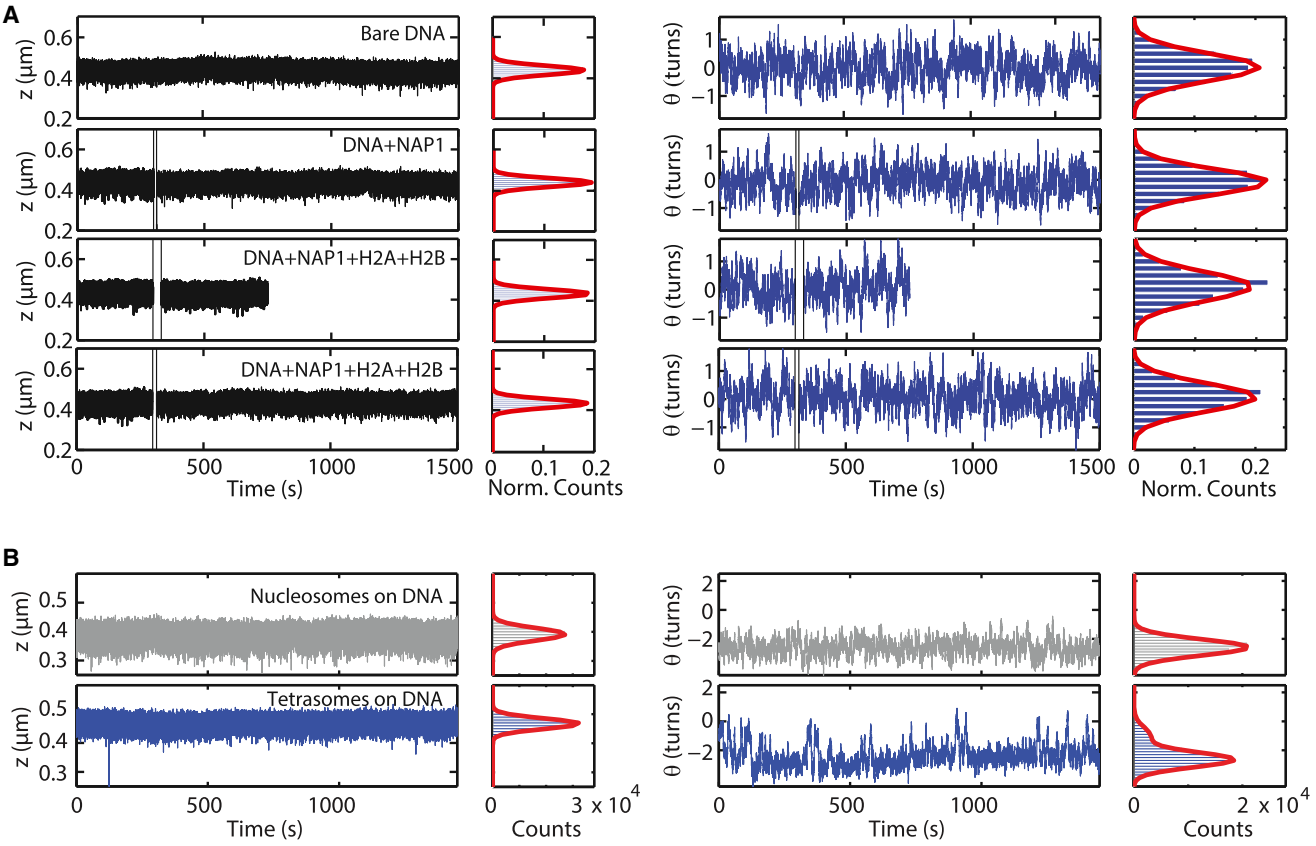

Figure 2. DNA Length and Linking Number Monitored as a Function of Time under Different Conditions

NAP1 by itself has no effect on bare DNA, nor is it capable of assembling H2A-H2B onto bare DNA. Loaded tetrasomes display dynamic changes in linking number.

(A) Top row: the DNA end-to-end extension z, at left, and the DNA linking number measured by monitoring bead rotations θ, at right, together with corresponding histograms, for bare DNA. The end-to-end extension and the linking number have mean values that are constant in time, with fluctuations about this mean measured to equal 22 nm and 0.48 turns, respectively. Second row: the same quantities as measured in the top row, but with the addition of 15 nM NAP1 at time $t = 300$ s. For both quantities, the mean value and the SD (21 nm and 0.46 turns, respectively) are unaltered by the addition of NAP1. Third row: the same quantities as measured in the top row, but with the addition of 0.3 nM NAP1 that had been preincubated for 30 min on ice with 0.5 nM of both H2A and H2B at time $t = 300$ s. This concentration is comparable to that used in the nucleosome assembly experiments (Figure 1). For both quantities, the mean value and the SD (21 nm and 0.52 turns, respectively) are unaltered by the addition of 0.3 nM NAP1 together with 0.5 nM of both H2A and H2B. Fourth row: the same quantities as measured in the top row, but with the addition of 3 nM NAP1 that had been preincubated for 30 min on ice with 5 nM H2A and 5 nM H2B at time $t = 300$ s. At this 10-fold excess concentration compared to that used in the third row, and in the nucleosome assembly experiments (Figure 1), the mean value and the SD (21 nm and 0.50 turns, respectively) are again unaltered. We furthermore note that flushing in of histones alone into the flow cell (i.e., in the absence of NAP1) does not lead to any assembly onto single molecules of DNA, but only to aggregation that results from nonspecific binding. Hence, we do not include time traces of DNA behavior in the presence of histones and the absence of NAP1.

(B) Extended observations of the behavior of DNA loaded with two nucleosomes (gray), and DNA loaded with three tetrasomes (blue) following assembly. The end-to-end length z, at left, and the angular coordinate θ, at right, are monitored simultaneously. Side panels show the corresponding histograms and fits to single or double Gaussian functions (red lines). In all cases, the mean extension is constant in time, with fluctuations about the mean arising from Brownian motion. Both bare DNA (top row in A) and DNA loaded with nucleosomes exhibit a fixed mean linking number in time, with comparable fluctuations about the mean ($\sigma = 0.46$, 0.55 turns, respectively). However, tetrasomes exhibit discrete changes in the linking number over time, as evidenced in the bimodal linking number distribution. The shift in angle between the two peaks of this distribution equals 1.6 ± 0.2 turns. In all panels, data are acquired at 100 Hz. See also Figure S1.

of the lifetimes can provide an estimate for the height of the energy barrier that lies between the left- and right-handed states, for which we find values in the range of $\sim$15–25 k_BT (Figure S2). Note that these values indicate an upper bound as a result of the finite bead response time ($\tau_{bead} \sim 1.5$ s) in our experimental configuration.

To investigate whether a tetrasome that flips between left- and right-handed states can accommodate the assembly of complete nucleosomes, we performed an experiment in which we first assembled H3-H4 on DNA, forming two tetrasomes that were observed to undergo continuous changes in the linking number (Figures 3E and S3). When we subsequently added histones H2A-H2B, we found that the flipping ceased abruptly, whereas the mean linking number decreased in two steps. The final linking number had a value of -2.4 turns, consistent with the assembly of two complete, left-handed nucleosomes. These

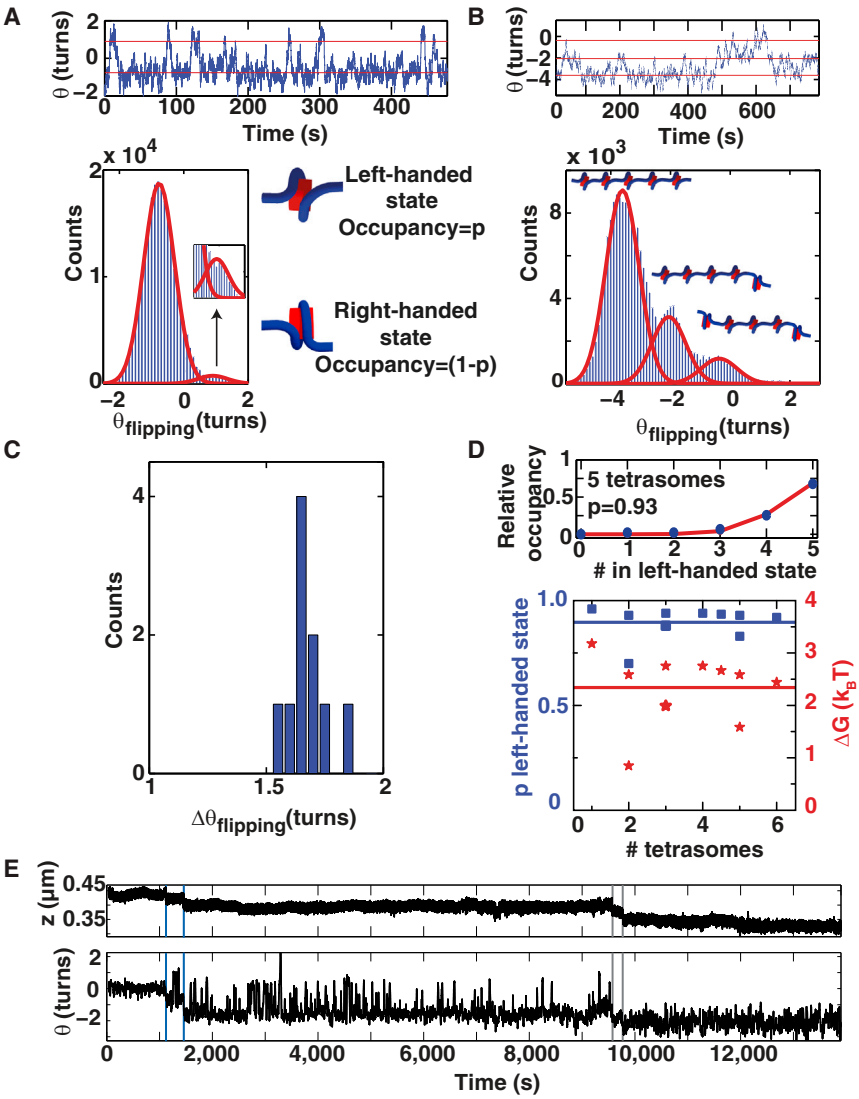

Figure 3. Tetrasomes Show Dynamic Changes in Linking Number

(A) Time trace and statistics of a DNA molecule loaded with a single tetrasome. The time trace shows the dynamics of linking number changes between $\theta = -0.8 \pm 0.1$ turns and $\theta = +0.9 \pm 0.1$ turns (values extracted from Gaussian fits to the histogram). Depictions of the corresponding left- and right-handed states are shown at the right, along with the accompanying probabilities assigned in a binomial model (see main text).

(B) Time trace and statistics of a DNA loaded with five tetramers. When all five tetrasomes were in the left-handed state, the lowest-measured value of the linking number was $\theta = -3.6$ turns (value extracted from Gaussian fitting to the histogram). When any one tetrasome flipped into the right-handed state, the linking number increased to $\theta = -2.0$ turns.

(C) Histogram of dynamical linking number steps observed following assembly of tetrasomes on distinct DNA molecules (n = 10), which yields a mean value of $< \Delta\theta_{flipping} > = 1.7 \pm 0.1$ turns.

(D) Determination of the probability p of finding a tetrasome in the left-handed state. The top panel shows the relative occupancies of each linking number state for a DNA loaded with five tetrasomes (deduced from Gaussian fits in B). A fit to the binomial model (solid red line) yields $p = 0.93$. The lower panel shows the values of p obtained in separate experiments in which different numbers of tetramers were loaded onto DNA (blue data; average value of p = 0.90). Using the relationship $\Delta G = -k_B T \ln((1/p) - 1)$, the values for p are used to extract the difference in energy between the left- and right-handed states (red stars; average value of $\Delta G = 2.3\ k_B T$).

(E) Assembly of two complete nucleosomes from two assembled tetrasomes. By flushing in NAP1 preincubated with H3-H4, we assembled two tetrasomes (blue lines mark the corresponding decreases in z and θ at t = 1,115 s and 1,454 s). Flipping behavior of the linking number was observed immediately following assembly and continued for 150 min. When we additionally flushed in histones NAP1 preincubated with H2A and H2B, we observed two additional assembly steps (gray lines mark the further decreases in both z and θ at t = 9,567 s and t = 9,770 s). The linking number subsequently remained stable at a mean value of −2.4 turns. See also Figures S2 and S3.

experiments establish that the dynamically flipping tetrasome is a viable intermediate in the assembly of nucleosomes.

Small Torques Can Drive Transitions in Tetrasomes and Nucleosomes

To study the fate of both nucleosomes and tetrasomes in response to physiologically relevant applied torques, we employed electromagnetic torque tweezers (eMTT) (Janssen et al., 2012) (Figure 4A). Reference measurements on bare DNA (Figure S4) showed that the application of turns to torsionally relaxed DNA initially left the DNA extension unchanged (Figure 4B, black), whereas the DNA twist increased, resulting in a linear buildup of torque (Figure 4C, black). From the slope of 1.5 ± 0.2 pN × nm/turn (n = 3) in this regime, we extract a torsional modulus C of 66 ± 8 nm, which is in good agreement with previous measurements (Mosconi et al., 2009; Figure 2F and Figure S12 in Lipfert et al. [2010], plus references therein). At a critical buckling torque of ~11 pN × nm, a decrease in the DNA extension z was observed as DNA buckled to form plectonemic supercoils, and beyond this no further torque buildup occurred (Figures 4B and 4C, black).

Torque measurements on DNA assembled with nucleosomes revealed three principal changes compared to bare DNA. First, we observed a decrease in the maximal extension due to the wrapping of DNA around the proteins (Vlijm et al., 2012) (Figure 4B, left, gray), as expected from FOMT measurements. Second, the maximum extension, which corresponds to the torsionally relaxed state of the tethered molecule, shifted toward negative turns (Figure 4B, left, gray) by $\Delta L_k = -1.2$ per assembled nucleosome, again in agreement with FOMT measurements. Third, the decreased slope in the linear regime of the torque-turns curve indicated a reduced torsional stiffness

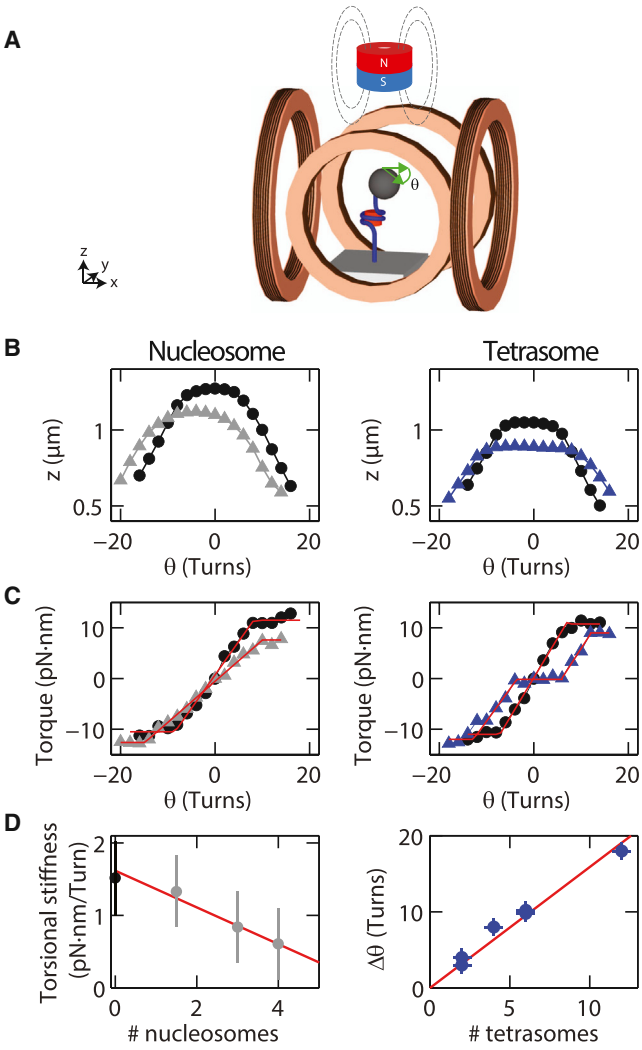

Figure 4. Torque Measurements on DNA with Nucleosomes and Tetrasomes

(A) Diagram of the eMTT configuration used in these experiments. The eMTT resembles the FOMT configuration but additionally has two pairs of Helmholtz coils placed around the flow cell to permit the application of torque.

(B) DNA end-to-end length *z* as a function of the number of rotations θ applied to the bead, for bare DNA (black circles in both panels; see also Figure S4A) and for the same DNA following assembly of three nucleosomes (left panel, gray triangles) or following the assembly of six tetrasomes (right panel, blue triangles).

(C) The torque stored in bare DNA (left and right panels, black circles), DNA loaded with nucleosomes (left panel, gray triangles), and tetrasomes (right panel, blue triangles) plotted as a function of the number of rotations, θ, relative to torsionally relaxed bare DNA (described in additional detail in Figure S4D). The slope of the red lines are fits to the data; the plateaus indicate the buckling torque.

(D) Left panel: buildup of torque per induced turn (deduced from the slopes of the linear response regions of the left panel in C) as a function of the number of assembled nucleosomes. A fit to a linear function yields a slope of −0.25 pN × nm/turn/nucleosome. Right panel: width of the plateau at near-zero torque (extracted from the right panel in C) as a function of the number of assembled tetrasomes. A fit to a linear function yields a plateau of 1.6 ± 0.1 turns/tetrasome. See also Figure S4.

(Figure 4C, left, gray; Figure S4F). Each nucleosome contributed to a change in the torsional stiffness of −0.25 pN × nm/turn, as shown by the one to one relationship between the effective torsional stiffness and the number of assembled nucleosomes (Figure 4D, left). This reduction in torsional stiffness reflects an absorption of torque by the nucleosome that delays the onset of DNA buckling by a substantial 1.3 ± 0.3 turns per assembled nucleosome, which is in agreement with earlier measurements (Bancaud et al., 2006; Bancaud et al., 2007). Because the measured torque-turns curve (Figure 4C, left, gray) directly showed that the buildup of torque occurred in a gradual and linear fashion (Bancaud et al., 2006, 2007), it appears that torque absorption by assembled nucleosomes occurs only through gradual conformational changes, either of the nucleosomes themselves or of the neighboring entry and exit DNA.

Torque measurements on DNA assembled with tetrasomes yielded additional differences compared to both bare DNA and DNA loaded with nucleosomes. Again, we observed a decrease in the maximal extension due to the wrapping of DNA around the proteins (Vlijm et al., 2012), as expected from FOMT measurements (Figure 4B, right, blue). However, for DNA loaded with tetrasomes the center of the rotation-extension response did not significantly shift compared to bare DNA and instead its width increased substantially (Figure 4B, right, blue; Vlijm et al., 2012). The origin of this response can be understood by examining the torque-turns curve (Figure 4C, right, blue), which now has a plateau with a near-zero slope around zero turns. This indicates that a negligibly low torque is sufficient to drive all tetrasomes into a left-handed configuration (when negative turns are imposed) or into a right-handed configuration (when positive turns are imposed). Indeed, because FOMT measurements revealed that the left- and right-handed states are separated by ~1.7 turns = 10.7 rad in angle and by ~2.3 k_BT = 9.4 pN × nm in energy, a mean torque of 9.4 pN × nm / 10.7 rad ~0.9 pN × nm should be sufficient to drive the transition between these two states. The observed near-zero slope around zero turns therefore agrees, within our experimental torque resolution of ~1 pN × nm, with the free energy difference between the two tetrasome states measured via FOMT. Further completing this picture, a linear fit of the plateau width versus the number of assembled tetrasomes yielded 1.6 ± 0.1 turns/tetrasome (Figure 4D, right, red line), and this is in good agreement with the direct measurement of $< \Delta\theta_{flipping} >$ from FOMT measurements.

DISCUSSION

We have performed a series of measurements that exploit the versatile measurement capabilities of the new FOMT technique to directly demonstrate the dynamical, continuous switching of a single tetrasome between two different states with respect to the handedness of the DNA path around the histone core. At the level of a single tetrasome, we have quantified this process in terms of linking number, underlying dynamics, interaction with additional histones such as H2A-H2B, and associated torque. Pioneering biochemical experiments by the Jackson and Prunell labs (Hamiche et al., 1996; Jackson, 1995) had previously demonstrated that tetramers have a high affinity for either positively or negatively supercoiled DNA. Their deduction that

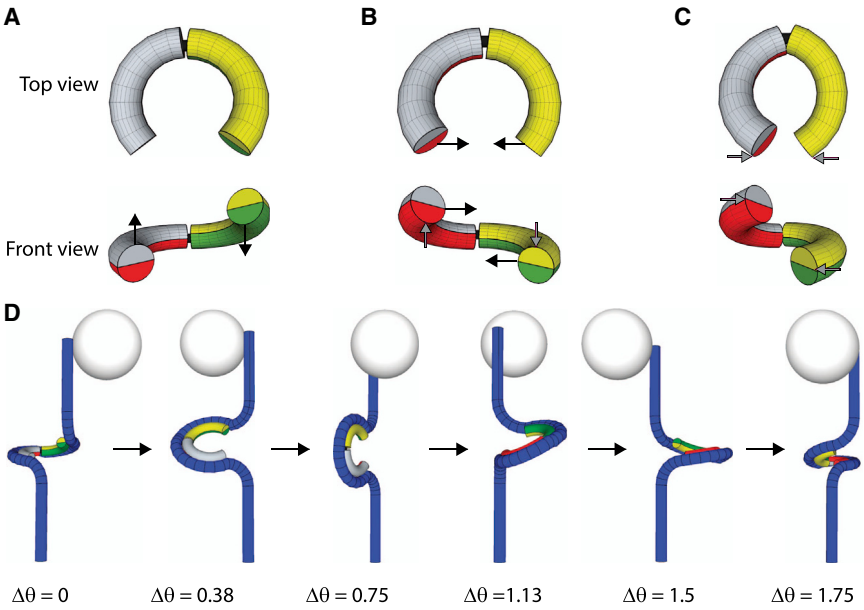

Figure 5. Model of the Tetrasome Conformations that Underlie the Observed Changes in Linking Number

In all panels, one (H3-H4) dimer is shown in yellow/green, the other (H3-H4) dimer is shown in red/gray. The H3-H3 interface that connects the two (H3-H4) dimers is represented by a hinge (black). The top and front views in (A)–(C) show the histone tetramer only, whereas (D) shows the complete tetrasome on the DNA (represented by the blue tube), together with the motion of the magnetic bead.

(A) Left-handed configuration of the tetrasome. The DNA is wrapped about the proteins in a left-handed fashion by −0.75 turns.

(B) Conformational change of the tetrasome from a left-handed to a right-handed helical wrapping of the DNA around the histones. Note that this flipping in linking number from −0.75 to +0.75 can be accomplished by a simple rotation of the hinge at the H3-H3 interface in which the yellow/green (H3-H4) dimer moves upward relative to the red-gray (H3-H4) dimer.

(C) Right-handed configuration of the tetrasome. Because the linking number was observed to flip between −0.75 and +1, the shape of the right-handed state is shown in a more compacted manner that allows the DNA to complete a full turn around the histone tetramer.

(D) Schematic representation of the bead rotation that is induced by the proposed conformational change of the tetrasome and the fixation of the DNA to the glass slide at the bottom. For visual clarity, we have drawn the tetrasome in the most conventional way; more likely, however, the energetics of DNA bending will cause the plane of the tetrasomes to adopt an oblique alignment rather than the horizontal one drawn.

See also Figure S5 and Movies S1 and S2.

tetrasomes with positive chirality were likely to form onto positively supercoiled minicircles suggested, when taken together with their observation that subsequent addition of topoisomerases could reduce the linking number by approximately two turns per tetrasome, a possible change in tetrasome handedness. Our results now directly report on the dynamics of the tetrasome loading process, demonstrating that tetrasomes do not require the presence of positive supercoils to adopt a configuration with positive handedness. Moreover, they provide direct evidence of spontaneously occurring dynamic transitions in the handedness of tetrasomes, indicating that the energy barrier separating such states of different handedness is sufficiently low to be overcome by thermal fluctuations. We observe in real time the accompanying changes in DNA length and angle, establishing that changes in tetrasome handedness do not involve unwrapping of the DNA and thereby constraining potential structural models of tetrasome flipping.

Based on our data, we propose a molecular model for the flipping of tetrasomes between left- and right-handed states (Figure 5). The left-handed tetrasome (Figure 5A) represents the lowest-energy state (reflecting its high p value) and has a linking number of −0.73 turns (Figure 1C), which is in close agreement with the −0.7 helical turns observed in crystal structures (Luger et al., 1997). To account for the ability of tetrasomes to modify their helicity without crossing significant energy barriers, we propose that the two H3-H4 dimers slightly rotate with respect to one another through the hinge that connects their interface (Figure 5B), a conformational change that allows the histone tetramer to maintain its DNA contacts. The resulting motion can be compared to that of the arms of a car driver who maintains her hands on the steering wheel while exiting from a right turn into a left turn (Figures 5A–5C and S5 and Movie S1). As suggested by crystal structure and bulk biochemical experiments (Hamiche et al., 1996; Hamiche and Richard-Foy, 1998; Luger et al., 1997), the H3-H3 interface may accommodate hinge rotation. With this motion complete, the tetrasome ends up in a right-handed state (Figure 5C) in which the measured linking number equals +1.0 ± 0.1 (reflected in a slightly more compact form of the two H3-H4 dimers; compare Figures 5B and 5C), allowing a full turn of DNA to wrap around the proteins. Such a compacted, right-handed tetrasome might not be able to form a stable structure with H2A-H2B dimers, thereby accounting for our experimental observation of exclusively left-handed assembled nucleosomes.

This molecular model of the tetrasome's conformational change accounts for the experimentally observed change in linking number. Because the DNA tether is rotationally clamped to the surface at its lower extremity, and because the entry and exit DNA cannot pass through one another, the change from left- to right-handed wrapping results in a rotation of the entire tetrasome. This subsequently brings about the observed rotation of the magnetic bead at the upper extremity of the DNA (Figure 5D; Movie S2). Notably, the model's assumption of the continuous maintenance of DNA contacts with the histone tetramer leaves the amount of "wrapped" DNA fixed, thereby accounting for the unchanged end-to-end distance of DNA observed during the flipping. Additionally, the model proposes that the H3-H4 dimers move relatively freely over minor

Please cite this article in press as: Vlijm et al., Nucleosome Assembly Dynamics Involve Spontaneous Fluctuations in the Handedness of Tetrasomes, Cell Reports (2015), http://dx.doi.org/10.1016/j.celrep.2014.12.022

distances, in accordance with our observation that the energy barrier between the left- and right-handed states is relatively small (approximately a few k_BT).

Our findings provide mechanistic insight into how nucleosomes, in particular, through their tetrasome intermediate, play important roles in the dissipation of the positive torsional stress, which in the cellular context can build up, e.g., ahead of transcribing RNA polymerases. A key ingredient herein is the documented evidence of the exchange of histones H2A and H2B, and hence of subnucleosome conformations, within chromatin. For example, from in vitro transcription assays on nucleosomal templates, it emerges that, whereas the transcription of highly expressed genes results in the eviction of a complete nucleosome (Kulaeva et al., 2010), transcription of moderately expressed genes may result in partial disassembly through the loss of either a single H2A-H2B dimer (Kireeva et al., 2002) or the loss of both, the latter notably under conditions of increased torsional stress or the presence of chaperones such as Nap1 (Levchenko et al., 2005; Sheinin et al., 2013). Additionally, numerous in vivo studies have revealed an increased exchange and hence mobility of H2A and H2B compared to that of H3 and H4 in transcriptionally active chromatin compared to that of H3 and H4 (Baer and Rhodes, 1983; Kimura and Cook, 2001; Thiriet and Hayes, 2006), as well as roles for many remodelers in the release and exchange of H2A and H2B (Burgess and Zhang, 2013; Mazurkiewicz et al., 2006). Visualization of transcriptionally active nucleosomes extracted from human cells revealed extended U-shaped particles early on (Bazett-Jones et al., 1996), with subsequent studies reporting subnucleosome conformations such as hexasomes and tetrasomes occupying genes during active transcription, again through preferential loss of H2A and/or H2B (Cole et al., 2014; Thiriet and Hayes, 2006). Thus, numerous lines of evidence suggest that tetrasomes exist within transcriptionally active genes, at least temporarily.

This conformational plasticity within chromatin, together with our results indicating different responses of nucleosomes and tetrasomes to torque, may well impact the motion of RNA polymerase. We have shown that nucleosomes are capable of undergoing gradual conformational changes in response to applied torques, but that tetrasomes undergo complete changes in chirality, even in the absence of torque. These results suggest that once tetrasomes are formed during transcription, they should have the ability to act as "torque buffer" in vivo by switching between left- and right-handed chirality. This possibility has been suggested by others (Alilat et al., 1999; Hamiche and Richard-Foy, 1998) but is made quantitatively plausible by our measurements that demonstrate that there is no large energy barrier separating the two tetrasome chiralities that would prevent tetrasomes from functioning as a "twist reservoir". Ahead of the transcription machinery, each tetrasome could simply absorb 1.7 positive turns by undergoing conformational changes from a left- to a right-handed state and preventing buildup of positive torque. In the wake of an RNA polymerase, such tetrasomes could then repopulate the left-handed state, absorbing 1.7 negative turns. Interestingly, tetrasomes could fulfill this role while remaining on their genomic site as markers of nucleosome positioning, permitting the redocking of the H2A-H2B dimers once they revert to left-handed states (Jorcano and Ruiz-Carrillo, 1979) and allowing chromatin to rapidly readopt its role in DNA compaction. It remains to be seen whether tetrasomes are unique in their ability to dynamically switch DNA wrapping directionality, or whether other subnucleosome conformations such as hexasomes could adopt similar roles (Arimura et al., 2012; Lavelle and Prunell, 2007). Furthermore, the roles of histone modifications or tails in the overall determination of chromatin's torsional response merit investigation in future experiments (Sivolob et al., 2000; Zheng and Hayes, 2003).

EXPERIMENTAL PROCEDURES

Single-Molecule Instrumentation

The traces monitoring NAP1-assisted nucleosome and tetrasome assembly via changes in extension and linking number, as well as any subsequent dynamics in linking number, were measured using the Freely Orbiting Magnetic Tweezers (FOMT) (Lipfert et al., 2011). The torque measurements were carried out in the Electromagnetic Torque Tweezers (eMTT) (Janssen et al., 2012). All measurements were performed at 21°C at an acquisition frequency of 100 Hz. Videos of the bead motion for a bare DNA tether and for a DNA tether with assembled tetrasomes assembled are shown in Movies S3 and S4.

Protein Expression and Purification

Recombinant *Drosophila* core histones were expressed in *E. coli* Bl21(DE3) Rosetta (Novagen) and purified as described in Levenstein and Kadonaga (2002), with the distinction that the purification procedure for the H3/H4 dimers was identical to that of the H2A/H2B dimers. Expression plasmids were a kind gift of J. Kadonaga. Concentrations of core histones were determined by SDS-PAGE and Coomassie staining as well as calculated from A280 measurements using the known absorption coefficients of *Drosophila* histones (Supplemental Experimental Procedures) and equimolar amounts were combined to obtain octamers. Recombinant *Drosophila* NAP1 was purified according to Lusser et al. (2005).

Flow Cell Passivation and Buffer Conditions

In all experiments, we used a buffer consisting of 50 mM KCl, 25 mM HEPES-KOH (pH 7.6), 0.1 mM EDTA, 0.025% polyethylene glycol (PEG), 0.025% polyvinyl alcohol (PVOH) for crowding, and 0.1 mg/ml BSA for crowding and to prevent nonspecific binding of the histones to the surface. For the tetrasome assembly experiments, 200 nM NAP1, 70 nM H3, and 70 nM H4 were preincubated, for the nucleosome assembly experiments, and 260 nM NAP1, 220 nM H2A, 220 nM H2B, 90 nM H3, and 90 nM H4 were preincubated for 30 min on ice. The preincubation buffer contained 50 mM KCl, 25 mM HEPES (pH 7.6), 0.1 mM EDTA, 0.25% PEG, 0.25% PVOH, and 1 mg/ml BSA. Just before flushing in, the protein concentration was lowered by about 1,000 times.

DNA Constructs

We used double-stranded DNA molecules of both 1.9 and 3.4 kbp in length. Both 1.9 and 3.4 kbp DNA molecules were used in the FOMT experiments, whereas only 3.4 kbp DNA molecules were employed in the eMTT experiments. To attach the DNA molecules to the glass surface and the bead, their extremities contained multiple digoxigenin molecules to one end and multiple biotin molecules at the other end. The DNA molecules used did not contain nucleosome positioning sequences. In the FOMT experiments, we used 0.5 μm diameter beads (Ademtech), whereas in the eMTT experiments we used 0.7 μm diameter beads (MagSense).

SUPPLEMENTAL INFORMATION

Supplemental Information includes Supplemental Experimental Procedures, five figures, and four movies and can be found with this article online at http://dx.doi.org/10.1016/j.celrep.2014.12.022.

AUTHOR CONTRIBUTIONS

R.V., M.L., J.L., C.D., and N.H.D. planned the experiments. A.L. provided all purified proteins used. R.V. and M.L. performed the experiments. R.V., M.L., and J.L. analyzed the data. R.V., M.L., J.L., A.L., C.D., and N.H.D. wrote the manuscript.

ACKNOWLEDGMENTS

We thank Tessa Jager for help with preliminary experiments. This work was supported by the Netherlands Organisation for Scientific Research (NWO; to J.L.), FWF START Y275 B12 (to A.L.), the Foundation for Fundamental Research on Matter (FOM; to C.D.), the European Research Council for ERC Advanced Grant NanoForBio (to C.D.), the European Research Council for ERC Starting Grant DynGenome (to N.H.D.), and the European Community's Seventh Framework Programme FP7/2007–2013 under grant agreement no. 241548 (MitoSys; to N.H.D.).

Received: August 29, 2014
Revised: November 4, 2014
Accepted: December 10, 2014
Published: January 8, 2015

REFERENCES

Alilat, M., Sivolob, A., Révet, B., and Prunell, A. (1999). Nucleosome dynamics. Protein and DNA contributions in the chiral transition of the tetrasome, the histone (H3-H4)2 tetramer-DNA particle. J. Mol. Biol. *291*, 815–841.

Andrews, A.J., Chen, X., Zevin, A., Stargell, L.A., and Luger, K. (2010). The histone chaperone Nap1 promotes nucleosome assembly by eliminating non-nucleosomal histone DNA interactions. Mol. Cell *37*, 834–842.

Arimura, Y., Tachiwana, H., Oda, T., Sato, M., and Kurumizaka, H. (2012). Structural analysis of the hexasome, lacking one histone H2A/H2B dimer from the conventional nucleosome. Biochemistry *51*, 3302–3309.

Asahara, H., Tartare-Deckert, S., Nakagawa, T., Ikehara, T., Hirose, F., Hunter, T., Ito, T., and Montminy, M. (2002). Dual roles of p300 in chromatin assembly and transcriptional activation in cooperation with nucleosome assembly protein 1 in vitro. Mol. Cell. Biol. *22*, 2974–2983.

Baer, B.W., and Rhodes, D. (1983). Eukaryotic RNA polymerase II binds to nucleosome cores from transcribed genes. Nature *301*, 482–488.

Bancaud, A., Conde e Silva, N., Barbi, M., Wagner, G., Allemand, J.F., Mozziconacci, J., Lavelle, C., Croquette, V., Victor, J.M., Prunell, A., and Viovy, J.L. (2006). Structural plasticity of single chromatin fibers revealed by torsional manipulation. Nat. Struct. Mol. Biol. *13*, 444–450.

Bancaud, A., Wagner, G., Conde E Silva, N., Lavelle, C., Wong, H., Mozziconacci, J., Barbi, M., Sivolob, A., Le Cam, E., Mouawad, L., et al. (2007). Nucleosome chiral transition under positive torsional stress in single chromatin fibers. Mol. Cell *27*, 135–147.

Bazett-Jones, D.P., Mendez, E., Czarnota, G.J., Ottensmeyer, F.P., and Allfrey, V.G. (1996). Visualization and analysis of unfolded nucleosomes associated with transcribing chromatin. Nucleic Acids Res. *24*, 321–329.

Bell, O., Tiwari, V.K., Thomä, N.H., and Schübeler, D. (2011). Determinants and dynamics of genome accessibility. Nat. Rev. Genet. *12*, 554–564.

Blosser, T.R., Yang, J.G., Stone, M.D., Narlikar, G.J., and Zhuang, X. (2009). Dynamics of nucleosome remodelling by individual ACF complexes. Nature *462*, 1022–1027.

Brower-Toland, B.D., Smith, C.L., Yeh, R.C., Lis, J.T., Peterson, C.L., and Wang, M.D. (2002). Mechanical disruption of individual nucleosomes reveals a reversible multistage release of DNA. Proc. Natl. Acad. Sci. USA *99*, 1960–1965.

Burgess, R.J., and Zhang, Z. (2013). Histone chaperones in nucleosome assembly and human disease. Nat. Struct. Mol. Biol. *20*, 14–22.

Chien, F.T., and van Noort, J. (2009). 10 years of tension on chromatin: results from single molecule force spectroscopy. Curr. Pharm. Biotechnol. *10*, 474–485.

Choy, J.S., and Lee, T.H. (2012). Structural dynamics of nucleosomes at single-molecule resolution. Trends Biochem. Sci. *37*, 425–435.

Clapier, C.R., and Cairns, B.R. (2009). The biology of chromatin remodeling complexes. Annu. Rev. Biochem. *78*, 273–304.

Claudet, C., Angelov, D., Bouvet, P., Dimitrov, S., and Bednar, J. (2005). Histone octamer instability under single molecule experiment conditions. J. Biol. Chem. *280*, 19958–19965.

Cole, H.A., Ocampo, J., Iben, J.R., Chereji, R.V., and Clark, D.J. (2014). Heavy transcription of yeast genes correlates with differential loss of histone H2B relative to H4 and queued RNA polymerases. Nucleic Acids Res. *42*, 12512–12522.

Gansen, A., Valeri, A., Hauger, F., Felekyan, S., Kalinin, S., Tóth, K., Langowski, J., and Seidel, C.A. (2009). Nucleosome disassembly intermediates characterized by single-molecule FRET. Proc. Natl. Acad. Sci. USA *106*, 15308–15313.

Hall, M.A., Shundrovsky, A., Bai, L., Fulbright, R.M., Lis, J.T., and Wang, M.D. (2009). High-resolution dynamic mapping of histone-DNA interactions in a nucleosome. Nat. Struct. Mol. Biol. *16*, 124–129.

Hamiche, A., and Richard-Foy, H. (1998). The switch in the helical handedness of the histone (H3-H4)2 tetramer within a nucleoprotein particle requires a re-orientation of the H3-H3 interface. J. Biol. Chem. *273*, 9261–9269.

Hamiche, A., Carot, V., Alilat, M., De Lucia, F., O'Donohue, M.F., Revet, B., and Prunell, A. (1996). Interaction of the histone (H3-H4)2 tetramer of the nucleosome with positively supercoiled DNA minicircles: potential flipping of the protein from a left- to a right-handed superhelical form. Proc. Natl. Acad. Sci. USA *93*, 7588–7593.

Ito, T., Bulger, M., Kobayashi, R., and Kadonaga, J.T. (1996). Drosophila NAP-1 is a core histone chaperone that functions in ATP-facilitated assembly of regularly spaced nucleosomal arrays. Mol. Cell. Biol. *16*, 3112–3124.

Jackson, V. (1995). Preferential binding of histones H3 and H4 to highly positively coiled DNA. Biochemistry *34*, 10607–10619.

Janssen, X.J., Lipfert, J., Jager, T., Daudey, R., Beekman, J., and Dekker, N.H. (2012). Electromagnetic torque tweezers: a versatile approach for measurement of single-molecule twist and torque. Nano Lett. *12*, 3634–3639.

Jiang, C., and Pugh, B.F. (2009). Nucleosome positioning and gene regulation: advances through genomics. Nat. Rev. Genet. *10*, 161–172.

Jorcano, J.L., and Ruiz-Carrillo, A. (1979). H3.H4 tetramer directs DNA and core histone octamer assembly in the nucleosome core particle. Biochemistry *18*, 768–774.

Kaplan, N., Moore, I.K., Fondufe-Mittendorf, Y., Gossett, A.J., Tillo, D., Field, Y., LeProust, E.M., Hughes, T.R., Lieb, J.D., Widom, J., and Segal, E. (2009). The DNA-encoded nucleosome organization of a eukaryotic genome. Nature *458*, 362–366.

Kimura, H., and Cook, P.R. (2001). Kinetics of core histones in living human cells: little exchange of H3 and H4 and some rapid exchange of H2B. J. Cell Biol. *153*, 1341–1353.

Kireeva, M.L., Walter, W., Tchernajenko, V., Bondarenko, V., Kashlev, M., and Studitsky, V.M. (2002). Nucleosome remodeling induced by RNA polymerase II: loss of the H2A/H2B dimer during transcription. Mol. Cell *9*, 541–552.

Kornberg, R.D. (1977). Structure of chromatin. Annu. Rev. Biochem. *46*, 931–954.

Kruithof, M., Chien, F.T., Routh, A., Logie, C., Rhodes, D., and van Noort, J. (2009). Single-molecule force spectroscopy reveals a highly compliant helical folding for the 30-nm chromatin fiber. Nat. Struct. Mol. Biol. *16*, 534–540.

Kulaeva, O.I., Hsieh, F.K., and Studitsky, V.M. (2010). RNA polymerase complexes cooperate to relieve the nucleosomal barrier and evict histones. Proc. Natl. Acad. Sci. USA *107*, 11325–11330.

Lavelle, C., and Prunell, A. (2007). Chromatin polymorphism and the nucleosome superfamily: a genealogy. Cell Cycle *6*, 2113–2119.

Please cite this article in press as: Vlijm et al., Nucleosome Assembly Dynamics Involve Spontaneous Fluctuations in the Handedness of Tetrasomes, Cell Reports (2015), http://dx.doi.org/10.1016/j.celrep.2014.12.022

Lee, J.Y., and Greene, E.C. (2011). Assembly of recombinant nucleosomes on nanofabricated DNA curtains for single-molecule imaging. Methods Mol. Biol. *778*, 243–258.

Levchenko, V., Jackson, B., and Jackson, V. (2005). Histone release during transcription: displacement of the two H2A-H2B dimers in the nucleosome is dependent on different levels of transcription-induced positive stress. Biochemistry *44*, 5357–5372.

Levenstein, M.E., and Kadonaga, J.T. (2002). Biochemical analysis of chromatin containing recombinant Drosophila core histones. J. Biol. Chem. *277*, 8749–8754.

Li, G., Levitus, M., Bustamante, C., and Widom, J. (2005). Rapid spontaneous accessibility of nucleosomal DNA. Nat. Struct. Mol. Biol. *12*, 46–53.

Lipfert, J., Kerssemakers, J.W., Jager, T., and Dekker, N.H. (2010). Magnetic torque tweezers: measuring torsional stiffness in DNA and RecA-DNA filaments. Nat. Methods *7*, 977–980.

Lipfert, J., Wiggin, M., Kerssemakers, J.W., Pedaci, F., and Dekker, N.H. (2011). Freely orbiting magnetic tweezers to directly monitor changes in the twist of nucleic acids. Nat. Commun. *2*, 439.

Liu, L.F., and Wang, J.C. (1987). Supercoiling of the DNA template during transcription. Proc. Natl. Acad. Sci. USA *84*, 7024–7027.

Luger, K., Mäder, A.W., Richmond, R.K., Sargent, D.F., and Richmond, T.J. (1997). Crystal structure of the nucleosome core particle at 2.8 A resolution. Nature *389*, 251–260.

Luger, K., Rechsteiner, T.J., and Richmond, T.J. (1999). Preparation of nucleosome core particle from recombinant histones. Methods Enzymol. *304*, 3–19.

Lusser, A., Urwin, D.L., and Kadonaga, J.T. (2005). Distinct activities of CHD1 and ACF in ATP-dependent chromatin assembly. Nat. Struct. Mol. Biol. *12*, 160–166.

Mazurkiewicz, J., Kepert, J.F., and Rippe, K. (2006). On the mechanism of nucleosome assembly by histone chaperone NAP1. J. Biol. Chem. *281*, 16462–16472.

Mihardja, S., Spakowitz, A.J., Zhang, Y., and Bustamante, C. (2006). Effect of force on mononucleosomal dynamics. Proc. Natl. Acad. Sci. USA *103*, 15871–15876.

Mosconi, F., Allemand, J.F., Bensimon, D., and Croquette, V. (2009). Measurement of the torque on a single stretched and twisted DNA using magnetic tweezers. Phys. Rev. Lett. *102*, 078301.

Nakagawa, T., Bulger, M., Muramatsu, M., and Ito, T. (2001). Multistep chromatin assembly on supercoiled plasmid DNA by nucleosome assembly protein-1 and ATP-utilizing chromatin assembly and remodeling factor. J. Biol. Chem. *276*, 27384–27391.

Okuwaki, M., Kato, K., and Nagata, K. (2010). Functional characterization of human nucleosome assembly protein 1-like proteins as histone chaperones. Genes Cells *15*, 13–27.

Olins, A.L., and Olins, D.E. (1974). Spheroid chromatin units (v bodies). Science *183*, 330–332.

Park, Y.J., Dyer, P.N., Tremethick, D.J., and Luger, K. (2004). A new fluorescence resonance energy transfer approach demonstrates that the histone variant H2AZ stabilizes the histone octamer within the nucleosome. J. Biol. Chem. *279*, 24274–24282.

Peterson, C.L. (2008). Salt gradient dialysis reconstitution of nucleosomes. CSH Protoc. *2008*, pdb. prot5113.

Peterson, S., Danowit, R., Wunsch, A., and Jackson, V. (2007). NAP1 catalyzes the formation of either positive or negative supercoils on DNA on basis of the dimer-tetramer equilibrium of histones H3/H4. Biochemistry *46*, 8634–8646.

Sheinin, M.Y., Li, M., Soltani, M., Luger, K., and Wang, M.D. (2013). Torque modulates nucleosome stability and facilitates H2A/H2B dimer loss. Nat. Commun. *4*, 2579.

Simon, M., North, J.A., Shimko, J.C., Forties, R.A., Ferdinand, M.B., Manohar, M., Zhang, M., Fishel, R., Ottesen, J.J., and Poirier, M.G. (2011). Histone fold modifications control nucleosome unwrapping and disassembly. Proc. Natl. Acad. Sci. USA *108*, 12711–12716.

Sivolob, A., De Lucia, F., Alilat, M., and Prunell, A. (2000). Nucleosome dynamics. VI. Histone tail regulation of tetrasome chiral transition. A relaxation study of tetrasomes on DNA minicircles. J. Mol. Biol. *295*, 55–69.

Strick, T.R., Allemand, J.F., Bensimon, D., Bensimon, A., and Croquette, V. (1996). The elasticity of a single supercoiled DNA molecule. Science *271*, 1835–1837.

Struhl, K., and Segal, E. (2013). Determinants of nucleosome positioning. Nat. Struct. Mol. Biol. *20*, 267–273.

Thåström, A., Lowary, P.T., Widlund, H.R., Cao, H., Kubista, M., and Widom, J. (1999). Sequence motifs and free energies of selected natural and non-natural nucleosome positioning DNA sequences. J. Mol. Biol. *288*, 213–229.

Thiriet, C., and Hayes, J.J. (2006). Histone dynamics during transcription: exchange of H2A/H2B dimers and H3/H4 tetramers during pol II elongation. Results Probl. Cell Differ. *41*, 77–90.

Torigoe, S.E., Urwin, D.L., Ishii, H., Smith, D.E., and Kadonaga, J.T. (2011). Identification of a rapidly formed nonnucleosomal histone-DNA intermediate that is converted into chromatin by ACF. Mol. Cell *43*, 638–648.

Visnapuu, M.L., and Greene, E.C. (2009). Single-molecule imaging of DNA curtains reveals intrinsic energy landscapes for nucleosome deposition. Nat. Struct. Mol. Biol. *16*, 1056–1062.

Vlijm, R., Smitshuijzen, J.S., Lusser, A., and Dekker, C. (2012). NAP1-assisted nucleosome assembly on DNA measured in real time by single-molecule magnetic tweezers. PLoS ONE *7*, e46306.

Zentner, G.E., and Henikoff, S. (2013). Regulation of nucleosome dynamics by histone modifications. Nat. Struct. Mol. Biol. *20*, 259–266.

Zhang, Y., Moqtaderi, Z., Rattner, B.P., Euskirchen, G., Snyder, M., Kadonaga, J.T., Liu, X.S., and Struhl, K. (2009). Intrinsic histone-DNA interactions are not the major determinant of nucleosome positions in vivo. Nat. Struct. Mol. Biol. *16*, 847–852.

Zheng, C., and Hayes, J.J. (2003). Intra-and inter-nucleosomal protein-DNA interactions of the core histone tail domains in a model system. J. Biol. Chem. *278*, 24217–24224.

Zlatanova, J., Seebart, C., and Tomschik, M. (2007). Nap1: taking a closer look at a juggler protein of extraordinary skills. FASEB J. *21*, 1294–1310.

Cell Reports

Supplemental Information

Nucleosome Assembly Dynamics Involve Spontaneous Fluctuations in the Handedness of Tetrasomes

Rifka Vlijm, Mina Lee, Jan Lipfert, Alexandra Lusser, Cees Dekker, and Nynke H. Dekker

Supplemental Data

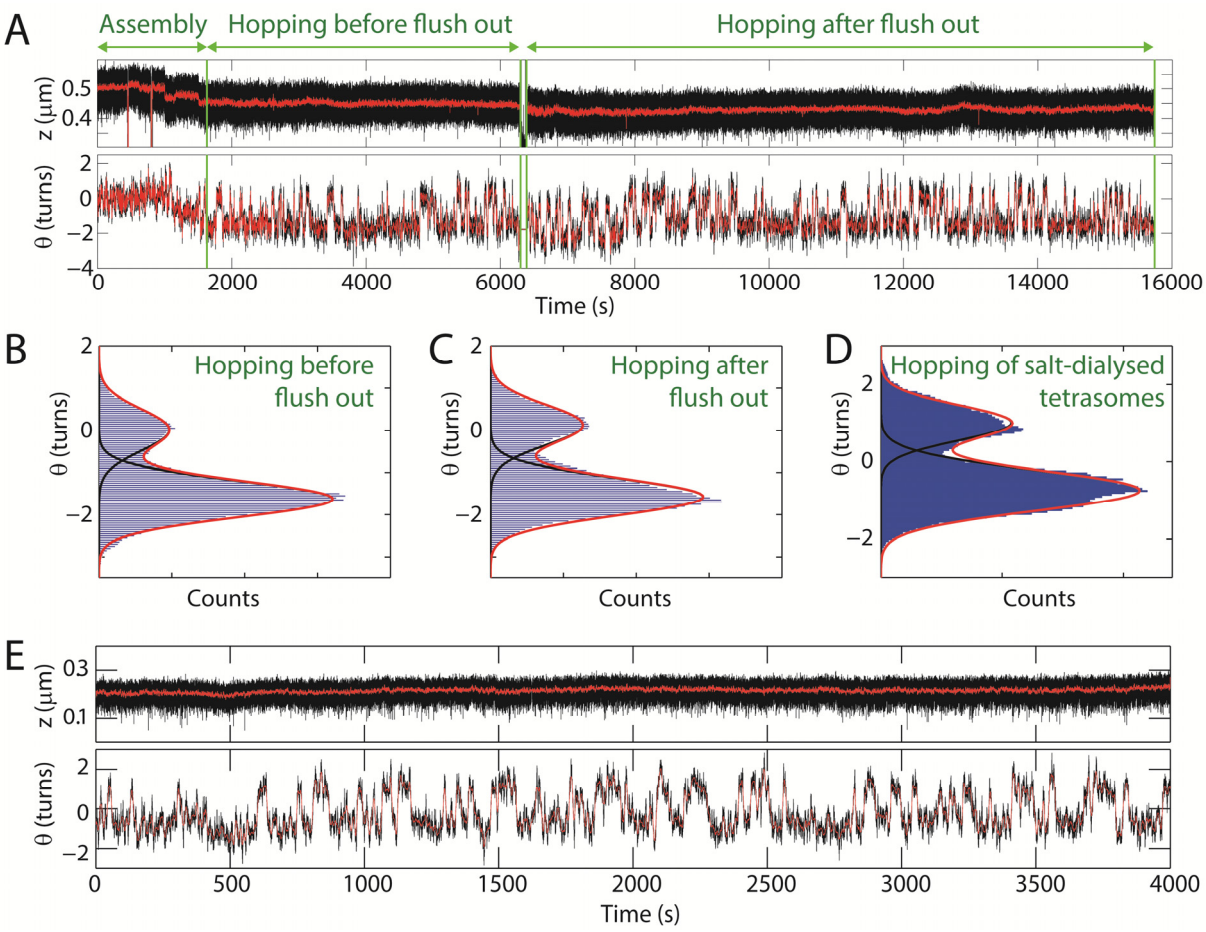

Figure S1, related to Figure 2. The observed spontaneous fluctuations in linking number do not require the continuous presence of unbound NAP1 and histones in the flow cell. (A) The DNA end-to-end extension *z*, top, and the DNA linking number measured by monitoring bead rotations θ, bottom. During the first 1650 s, flushing in of NAP1 preincubated with H3/H4 leads to the assembly of two complete tetrasomes. Between t = 1650-6249 s, the length of the DNA is constant while its linking number fluctuates due to the flipping between left-handed and right-handed tetrasomes. Between t = 6249-6335 s, 700 µl of buffer (equal to 7 cell volumes) was flushed through the flow cell to remove any unbound proteins. This washing step does not affect the length, the linking number, or, to any significant extent, the dynamics of loaded tetrasomes, demonstrating that the flipping of tetrasome handedness is independent

of the presence of free protein in solution. Data are acquired at 100 Hz, raw data shown in black. For clarity, moving averages are shown in red (averaging over 200, 800 points for the z, θ traces, respectively). (B) Histogram of the tether linking number following assembly but prior to flushing out the free proteins (t = 1650-6249 s). The centres of the two Gaussians are located at -1.63 and +0.01 turns, respectively. (C) Histogram of the tether linking number following flushing out of the free proteins (t = 6335-15740 s). The dynamics remain similar, and the centres of the two Gaussians are located at -1.58 and +0.12 turns, indicating that the flipping behaviour is unaffected by the removal of unbound proteins. (D,E) The length and angular coordinate of a single DNA molecule onto which tetrasomes were reconstituted via salt dialysis. Reconstitution was performed in bulk according to standardized protocols, and the resulting molecules were transferred to the flow cell for analysis at the single-molecule level. As in the case of DNA molecules that were loaded with tetrasomes by NAP1, we monitor the length z and angle θ of the molecule as a function of time. The accompanying histogram of the angular coordinate is shown in D). The z-coordinate remains fixed as a function of time. Conversely, the angular coordinate undergoes transitions between two distinct states. Fitting of the histogram of the angular coordinate indicates that these two states are separated by a change in linking number $\Delta Lk = 1.64 \pm 0.02$ turns.

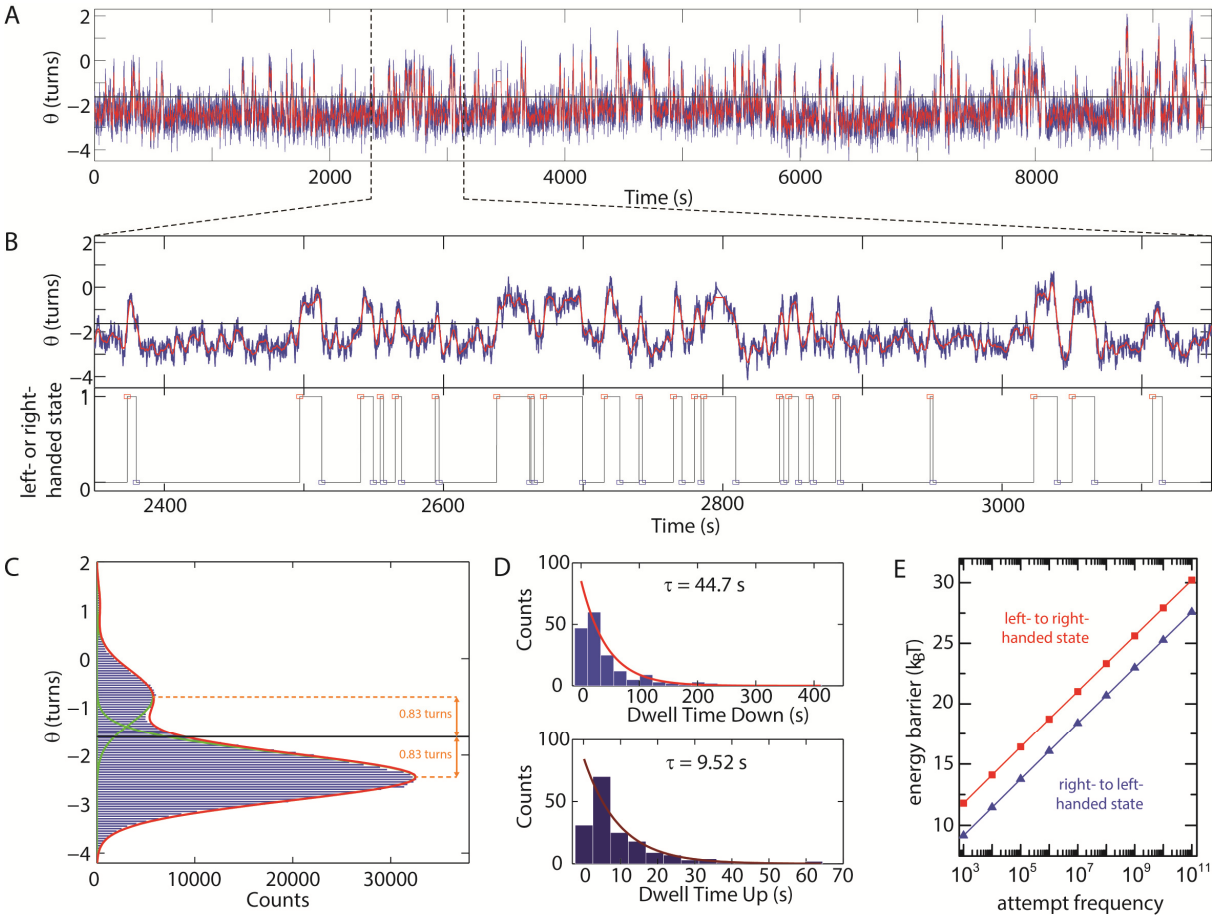

Figure S2, related to Figure 3. Analysis of the dwell times in the left- and right-handed state. (A) We measured the DNA linking number for 9452 s by monitoring bead rotations θ of a molecule following the assembly of three tetrasomes. Raw data acquired at 100 Hz shown in blue, data filtered by a 350-point (= 3.5 s) moving average shown in red. (B) To illustrate how accurately the smoothed curves follow the raw data, the top panel shows part of the data trace. To assign the tetrasomes to either a negative or positive state, we use a threshold whose value is set as described in C). For each filtered data point (red trace, upper panel B), we determined whether the tetrasomes were all in the left-handed state (lower panel B, threshold set at 0), or not (lower panel B, threshold set at 1). Since the probability that two or more of the tetrasomes occupy the positive state is only 1.3% (fraction of raw data points with linking number 0.17 or higher), each point above the threshold is considered to represent a single tetrasome in the right-handed state. The times between these switches of state are the lifetimes

in either state. (C) Histogram of the linking number of the raw data trace shown in A). Gaussian fits to the two most prominent peaks (green) yield centres at -2.45 and -0.79. Thus, the average linking number of a tetrasome a left–handed state in this dataset is -0.81 turns (in good agreement with data in Figure 1C, lower right panel), and $\Delta\theta_{flipping}$ = 1.66 turns (in good agreement with data in Figure 3C). The sum of the Gaussian fits is shown in red. The threshold that discriminates between (3,0) tetrasomes in the (left, right)-handed state versus (2,1) tetrasomes in the (left, right)-handed state is determined by the midpoint between the means extracted from the two largest Gaussian fits, and equals -1.62 turns. Data filtering is performed using a moving average of 350 points on the raw data acquired at 100 Hz, with results in a 2.5% detection rate of false positive state changes as determined using a reference trace of bare DNA. (D) Histograms of the lifetimes in the left- and right-handed states. The top panel shows the dwell times during which all three tetrasomes occupied the left-handed state, together with an exponential fit (red) with a characteristic time of 44.7 s. Thus, the characteristic time for a single tetrasome to occupy the left-handed state $\tau_{left\text{-}handed}$ equals 134.1 s. The lower panel shows the dwell times for a single tetrasome in the right-handed state, yielding $\tau_{right\text{-}handed}$ = 9.52 s. (E) The lifetimes of a single tetrasome in the left- and right-handed states can be plugged into an Arrhenius equation $\Gamma = \omega e^{-\Delta G^{\ddagger}/k_B T}$ to yield the height of the energy barrier that separates the left- and right-handed states; here, Γ is the overall hopping rate, ω is the attempt frequency of the tetrasome to flip from one state to the other, and $\Delta G^{\ddagger}$ is the height of the intervening energy barrier. While classical transition state theory assumes a value for ω ~10^{12} Hz, depending on the system in question its value can be many orders of magnitude smaller. For example, it is ~10^{9} Hz for the case of membrane proteins [S1] and it may well be even smaller for large nucleoprotein complexes such as the nucleosome. By scanning a range of values for ω between 10^{4}-10^{10} Hz and using our measured value for the overall hopping rate [S2, S3, S4], we estimate the height of the energy

barrier for going from the left-handed state to the right-handed state to lie between 14-28 k_BT. Similarly, we estimate the energy barrier for going from the right-handed state to the left-handed state to lie between 11-25 k_BT. Both ranges should be considered as an upper limits, since we cannot experimentally observe flipping times shorter than the bead response time, $\tau_{bead} \sim$ 1.5 s (Lipfert et al., 2011).

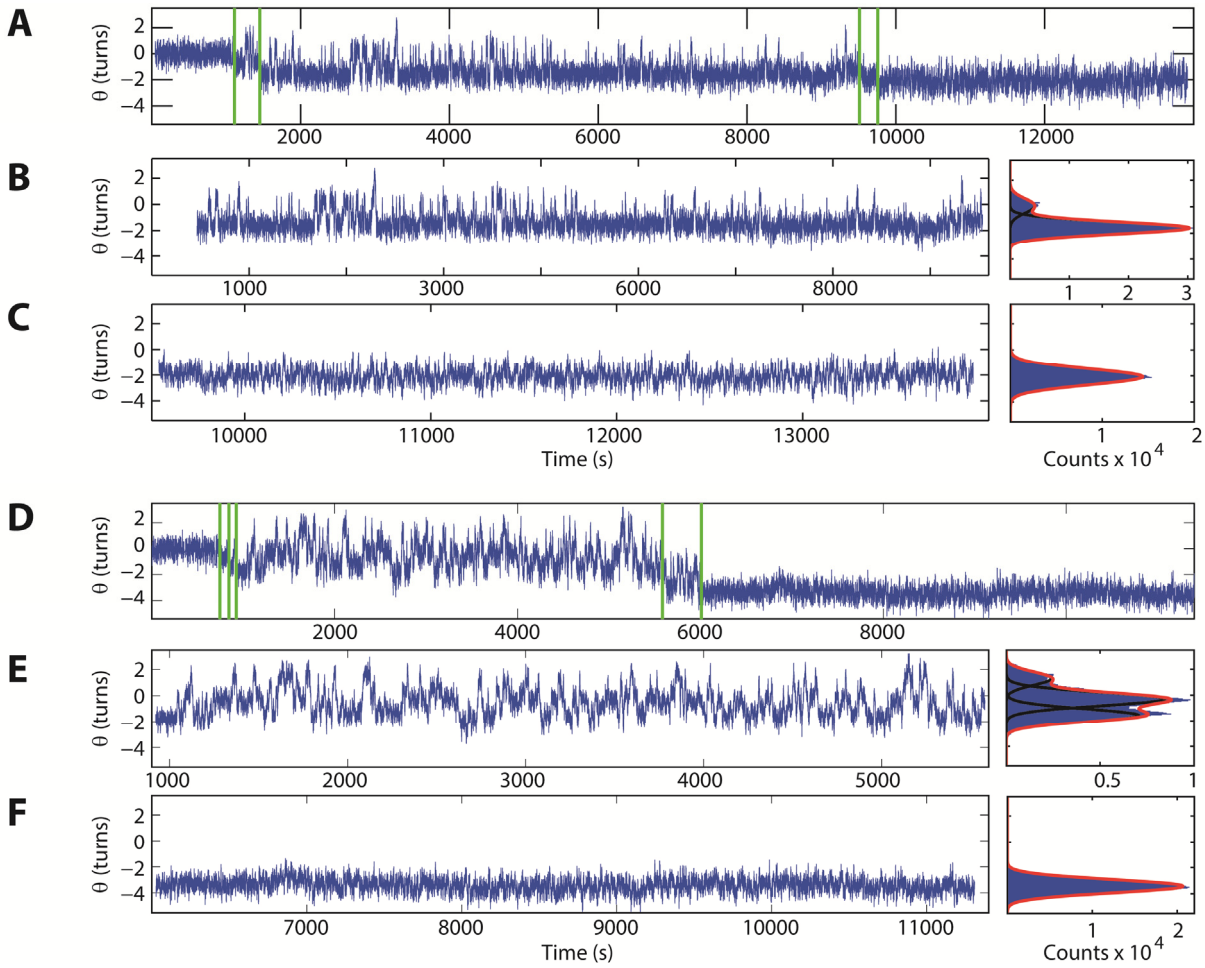

Figure S3, related to Figure 3. Assembly of tetrasomes, followed by nucleosome assembly by the addition of H2A/H2B. (A) (same data as Figure 3E) By flushing in NAP1 preincubated with H3-H4, we assembled two tetrasomes (green lines mark the corresponding decreases in angle at t = 1115 s and 1454 s). Flipping behavior of the linking number was observed immediately following assembly and continued for 150 min. When we additionally flushed in histones NAP1 preincubated with H2A and H2B, we observed two additional assembly steps (green lines mark the further decreases in angle at t = 9567 s and t = 9770 s). The linking number subsequently remained stable. (B) Part of the trace in A) with the tetrasomes assembled. The right panel shows the histogram of the angle with two Gaussian fits (black) and the sum of those fits (red).The centers of the Gaussian fits are at -1.6 and 0.1 turns. (C) Part of the trace in A) with nucleosomes assembled following addition of H2A-H2B. The

right panel shows the histogram of the angle, which fits to a single Gaussian with a center at -2.1 turns. (D) By flushing in NAP1 preincubated with H3-H4 (t = 700 s), we assembled three tetrasomes (green lines mark the corresponding decreases in angle at t = 750, 842 and 921 s). Flipping behavior of the linking number was observed immediately following assembly and continued for 78 min. When we additionally flushed in histones H2A and H2B preincubated with NAP1, we observed additional assembly (green lines mark the further decreases in angle between t = 5580 s and t = 6010 s). The linking number subsequently remained stable. (E) Part of the trace in D) with the tetrasomes assembled. The right panel shows the histogram of the angle with three Gaussian fits (black) and the sum of those fits (red). The centers of the Gaussian fits are at -1.6, -0.3 and 1.3 turns. (F) Part of the trace in D) with nucleosomes assembled following addition of H2A-H2B. The right panel shows the histogram of the angle, which fits to a single Gaussian with a center at -3.4 turns.

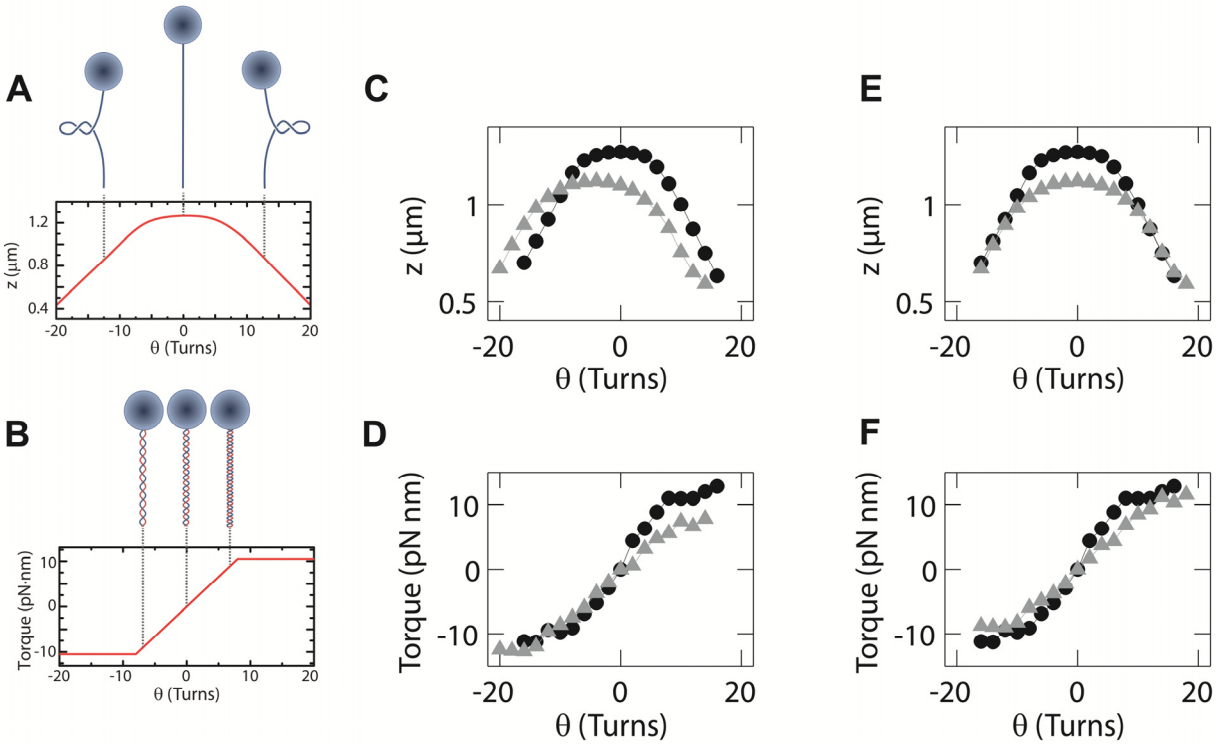

Figure S4, related to Figure 4. Response of DNA extension and torque to applied turns for bare DNA and DNA with nucleosomes. (A) Sketch of the response of bare DNA extension to applied turns at constant low force, together with illustrations of the tethered bare DNA. In the absence of applied turns, the DNA is in a torsionally relaxed state, which has a maximal extension. The application of a small number of positive or negative turns (here ~4, but in general dependent on the total length of the DNA) alters the twist in the DNA without significant changes in *z*. When a larger number of turns is applied, a buckling point is reached beyond which positive or negative plectonemes are formed, one for each extra turn. (B) Sketch of the response of stored torque in the DNA to applied turns at constant force, together with illustrations of the tethered bare DNA. As described in **a**, the initial application of turns to a rotationally relaxed DNA induces twist in the DNA. Negative turns result in under-winding of the (intrinsically positively twisted) DNA helix and positive turns result in over-winding of the DNA, as depicted. Relaxed DNA at 0 turns stores no torque, whereas the build-up of twist results in an accumulation of torque in the DNA. Once a critical torque has

been reached (corresponding to the buckling point in A), the twist no longer increases but instead the DNA buckles, and the value of the stored torque saturates. Both examples are sketches for a 3.4 kbp long DNA molecule under an applied stretching force of 0.7 pN. Panels (C,D) in this supplemental figure are identical to the two leftmost panels of Figure 4B,C in the main text. (C) The extension z of bare DNA (black circles) and of the same DNA following the assembly of three nucleosomes (grey triangles) as a function of applied turns θ at F = 0.7 pN. (D) The torque stored in bare DNA (black circles) and in DNA loaded with nucleosomes (grey triangles) as a function of applied turns. The applied turns in (C,D) are referenced with respect to the rotational offset of bare DNA, which was determined from the location in turns at which its extension was maximal at F = 0.3 pN. To facilitate comparison between the measurements of bare DNA and DNA loaded with nucleosomes, we have replotted this data relative to the rotational offset of DNA loaded with nucleosomes, which we have defined as the positions in turns of the maximal extension for this molecule (grey triangles in C). The results of this replotting are shown in (E,F). Note that an alteration of the angular offset also results in a corresponding shift in the measured torque values in F). In this way, one can more easily see that the slope of linear regime in the torque-turns response was decreased upon the assembly of nucleosomes indicating a reduced torsional stiffness (see main text) and that the values of the buckling torques at both negative and positive supercoiling were unaffected by nucleosome assembly.

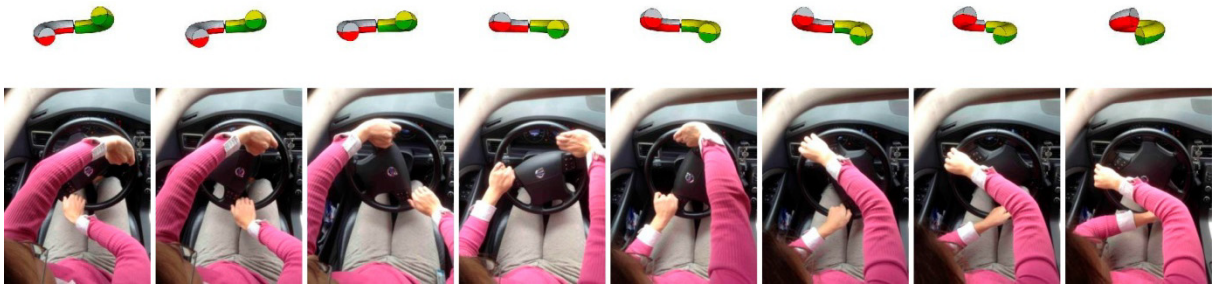

Figure S5, related to Figure 5. Toggling arms model. Stills of Supplementary movie 1: a car driver's arms with the hands on the steering wheel of a car. Illustrated are the similarities between the movement of the arms of a driver who maintains her hands on the steering wheel while exiting from a right turn into a left turn, and the histone tetramer in our model of tetrasome flipping (Figure 5). Note the different handedness of the arms at the start and finish of the turning process, where the arms have toggled from a right-handed to a left-handed configuration.

Movie S1, related to Figure 5. Toggling arms model. Video of a driver's arms with the hands on the steering wheel of a car. This video illustrates the similarities between the movement of the arms of a driver who maintains her hands on the steering wheel while exiting from a right turn into a left turn, and the histone tetramer in our model of tetrasome flipping (Figure 5). Note the different handedness of the arms at the start and finish of the turning process, where the arms have toggled from a right-handed to a left-handed configuration.

Movie S2, related to Figure 5. Molecular model. Video illustration the rotation of the tetrasome that results from the conformation change of the histone tetramer during flipping. Color notation follows that of Figure 5 (main text): DNA is shown in blue, one H3-H4 dimer in red/grey, and the other H3/H4 dimer in yellow/green. The black hinge represents the H3/H3 interface. At the top end of the DNA a bead is drawn (not to scale) in order to complete the illustration of our experimental configuration.

Movie S3, related to Experimental procedures. Angular motion of a bead tethered to bare DNA. Video showing the bead motion of a bare DNA tether. Images are acquired at 100 Hz. In the movie, counter-clockwise movement corresponds to positive (right-handed) rotation of the DNA while clockwise movement corresponds to negative (left-handed) rotation of the DNA. The thermal fluctuations of the angular coordinate are of the order of 1 turn ($\sigma = 0.5$ turns).

Movie S4, related to Experimental procedures. Angular motion of a bead tethered to DNA reconstituted with tetrasomes. Video showing bead motion of a DNA tether reconstituted with tetrasomes via salt-dialysis. Images are acquired at 100 Hz. In the movie, counter-clockwise movement corresponds to positive (right-handed) rotation of the DNA while clockwise

movement corresponds to negative (left-handed) rotation of the DNA. Consecutive ~1.7 turns in clockwise and counter-clockwise direction form the signature of flipping.

Supplemental Experimental Procedures: Description of tetramer assembly using bulk salt dialysis.

Salt dialysis of tetrasomes

The assembly of nucleosomes and tetrasomes through salt dialysis is a well-established method [S5, S6]. First, the histones and DNA are mixed in a high salt buffer. Next, the salt concentration was slowly reduced, in our case over a time period of 16 hours at 4°C. Finally the samples were stored until use in a low salt buffer at 4°C.

DNA constructs for salt dialysis of tetrasomes

The DNA with a tether length of 1.9 kb containing DIG-handles at one end and biotin-handles at the other end (see main text) gives a total DNA length of 3.2kb. Concentration: 2.7µg in 50µl buffer (20mM Tris, 1mM EDTA, 2M KCL).

Histone octamers

Drosophilla histones H3 and H4 are used, the same as used during NAP1-assisted tetramer assembly. Concentration: equimolar mix of 0.45µg/µl in buffer (20mM Tris, 1mM EDTA, 2M KCL).

Buffers

All the buffers fresh.

High salt buffer (250 ml)	20mM Tris-HCl (pH 7.5) 1mM EDTA 2M KCl 1mM DTT 0.5mM Benzamidine mQ
Low salt buffer (1L)	20mM Tris-HCl (pH 7.5) 1mM EDTA

	10mM KCl 1mM DTT 0.5mM benzamidine mQ
Assembly buffer (1ml)	20mM Tris-HCl (pH 7.5) 1mM EDTA 2M KCl 10mM DTT 0.5mM benzamidine mQ

Protocol

Step 1: Place the buffers without DTT and benzamidine at 4°C. When the temperature of 4°C is reached, finish the buffers by adding DTT and benzamidine.

Step 2: Rinse the dialysis cups (Thermo Scientific, #69550; 3.5K-MWCO) in 50°C warm mQ water for 10 minutes and remove leaking cups. Cool down in cold mQ.

Step 3: Use LoBind Eppendorf tubes to prevent protein loss due to sticking to the tubes.

Step 4: Prepare the histone-DNA mix. In our experiments, we do not aim for maximum number of tetrasomes, since we want to mimic the conditions of the NAP1-assisted assembly as close as possible. For this purpose we prepared the weight ratio of DNA : histones of 1 : 0.56. A total of 0.8µg of DNA, and 0.45µg of histones was mixed in the assembly buffer to add up to a total volume of 50µl and placed in a dialysis cup.

Step 5: Prepare the dialysis setup as shown in the figure below. A 250ml beaker with stir bar should be filled with high salt buffer and placed on a stirrer in a cold room with a temperature of 4°C. Two clean tubes should be attached to the inner wall of this beaker such that the ends nearly touch the bottom of the beaker. One of these tubes should go to a beaker containing the low-salt buffer and the other should go to a waste container, with a minimum volume of a litre. A peristaltic pump (Ismatec) is

set to pump low salt buffer into the dialysis beaker and, at the same rate, remove buffer from the dialysis beaker to the waste container.

Step 6: Place the dialysis cups in a floating device, and place this floating device into the beaker containing the high salt buffer. Start the stirring device and make sure the floater is free to rotate.

Step 7: Set the pump such that one litre is pumped over a time of 16 hours.

Step 8: When the dialysis is finished, write down the final volume in the individual dialysis cups and store the samples in a LoBind Eppendorf tube until use at 4°C.

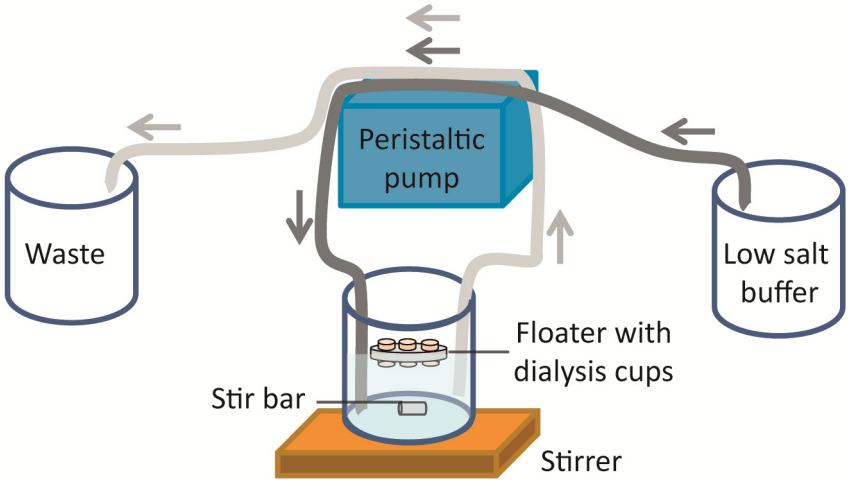

Schematic representation of the salt-dialysis setup. During a 60-hour dialysis at 4°C, the salt concentration is reduced from 2M to 10mM KCl.

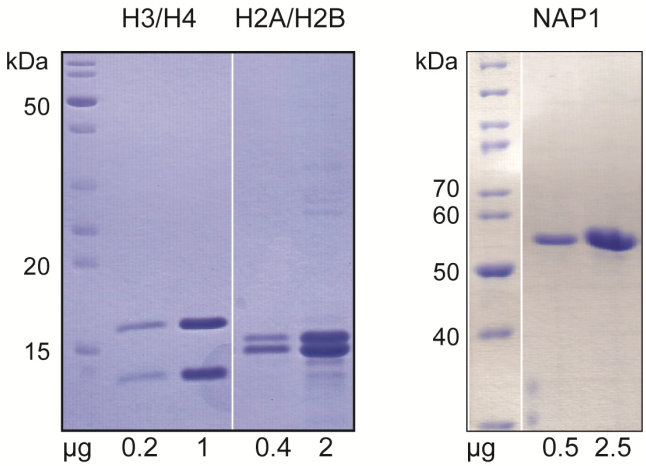

Coomassie staining of SDS polyacrylamide gel showing different concentrations of purified recombinant histones H3/H4 (0.2 and 1 μg), H2A/H2B (0.4 and 2 μg) and of purified recombinant NAP1 (0.5 and 2 μg). Protein marker II (Peqlab) was used as a molecular size marker and is shown in the leftmost lanes of both panels.

Supplemental References

[S1] Danelon, C., Brando, T., and Winterhalter, M. (2003). Probing the orientation of reconstituted maltoporin channels at the single-protein level. The Journal of biological chemistry *278*, 35542-35551.

[S2] Best, R.B., and Hummer, G. (2006). Diffusive model of protein folding dynamics with Kramers turnover in rate. Physical review letters *96*, 228104.

[S3] Chung, H.S., and Eaton, W.A. (2013). Single-molecule fluorescence probes dynamics of barrier crossing. Nature *502*, 685-688.

[S4] Soranno, A., Buchli, B., Nettels, D., Cheng, R.R., Muller-Spath, S., Pfeil, S.H., Hoffmann, A., Lipman, E.A., Makarov, D.E., and Schuler, B. (2012). Quantifying internal friction in unfolded and intrinsically disordered proteins with single-molecule spectroscopy. Proceedings of the National Academy of Sciences of the United States of America *109*, 17800-17806.

[S5] Lee, K.M., and Narlikar, G. (2001). Assembly of nucleosomal templates by salt dialysis. Current protocols in molecular biology / edited by Frederick M Ausubel [et al] Chapter 21, Unit 21 26.

[S6] Luger, K., Rechsteiner, T.J., and Richmond, T.J. (1999). Preparation of nucleosome core particle from recombinant histones. Methods in enzymology 304, 3-19.